

AD-A154 634

BEAM MODIFICATION FOR CANCER RADIATION THERAPY(U) AIR
FORCE INST OF TECH WRIGHT-PATERSON AFB OH SCHOOL OF
ENGINEERING J M KELLER MAR 85 AFIT/GEP/GNE/85M-10

1/1

UNCLASSIFIED

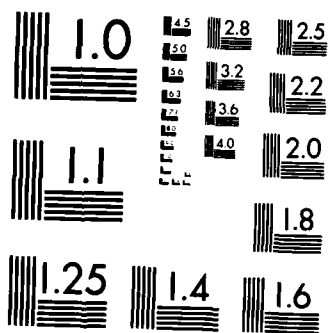
F/G 6/5

NL

END

FILED

DTIC



MICROCOPY RESOLUTION TEST CHART
NATIONAL BUREAU OF STANDARDS-1963-A

AD-A154 634



BEAM MODIFICATION
FOR CANCER RADIATION THERAPY

THESIS

Justin M. Keller, B.S.
Second Lieutenant, USAF

AFIT/GEP/GNE/85M-10

Acces
NTIS
DTIC
Unan
Just

This document has been approved
for public release and its
distribution is unlimited.

DEPARTMENT OF THE AIR FORCE
AIR UNIVERSITY

AIR FORCE INSTITUTE OF TECHNOLOGY

Wright-Patterson Air Force Base, Ohio

DTIC FILE COPY

DTIC
ELECTE
S JUN 4 1985
E

AFIT/GEP/GNE/85M-10

BEAM MODIFICATION
FOR CANCER RADIATION THERAPY

THESIS

Justin M. Keller, B.S.
Second Lieutenant, USAF

AFIT/GEP/GNE/85M-10



Accession For	
NTIS GRA&I	<input checked="" type="checkbox"/>
DTIC TAB	<input type="checkbox"/>
Unannounced	<input type="checkbox"/>
Justification	
By _____	
Distribution/	
Availability Codes	
Dist	Avail and/or Special
A/	

Approved for public release; distribution unlimited



AFIT/GEP/GNE/85M-10

BEAM MODIFICATION
FOR CANCER RADIATION THERAPY

THESIS

Presented to the Faculty of the School of Engineering
of the Air Force Institute of Technology
Air University
In Partial Fulfillment of the
Requirements for the Degree of
Master of Science in Nuclear Engineering

Justin M. Keller, B.S.
Second Lieutenant, USAF

March 1985

Approved for public release; distribution unlimited

Acknowledgements

This endeavor could not have seen fruition without the help of the Medical Center's health physicists: LtCol. John Swanson and Maj. John Ricci. Each of them endured countless inquiries and interruptions for the sake of this research. I would like to thank both of them for the advice, time, and patience they expended on my behalf.

I would like to thank Dr. George John for introducing me to this topic and for nudging us to an early start in our work. The additional effort paid off.

I also owe a debt of gratitude to my late grandmother, Mrs. Berniece Breeden, for teaching me to ask "Why?" and "Why not?" at the same time.

Finally, I would like to thank the producers of "The A-Team" for a welcome distraction on Tuesday evenings during this hectic time.

Justin Keller

Table of Contents

	Page
Acknowledgements	ii
List of Figures	iv
Abstract	vii
I. Introduction	1
II. Design Methodology	7
III. Results	20
IV. Conclusions	49
V. Recommendations	50
Appendix A: Effect of Contour on Beam Uniformity	52
Appendix B: Application to Non-planar Tumors	58
Appendix C: Outline of Irregular Field and External Beam Treatment Techniques	61
Appendix D: TLD Theory and Statistics	65
Appendix E: Sample Treatment Plans and Dose Profiles	69
Bibliography	77
Vita	78

List of Figures

Figure	Page
1. Placement of Compensator in Treatment Beam	3
2. Co-ordinate System with Respect to Patient Orientation	8
3. Typical CT Scan Slice	9
4. Normalized Dose Distribution at Tumor Plane	9
5. Lateral Dimensions of Modifier	12
6. The Alderson Rando Phantom	15
7. Chest Section from the Rando Phantom	17
8. The Cobalt-60 Treatment Machine	18
9. An Aluminum Block Beam Modifier	19
10. Dose Distribution in Rando Sections 11-18 from an Unmodified Anterior Beam	21
11. Dose Distribution in Rando Sections 11-18 with Higgins' Tissue Compensator in place	22
12. Dose Distribution in Rando Section 14 in Three Media	24
13. Normalized Dose Distribution in Three Rando Sections (Unmodified Anterior Narrow Beam)	26
14. Geometry for Modifier in z-direction	28
15. Normalized Dose Distribution in Three Rando Sections (Modifier in place)	30
16. Normalized Dose Distribution in Three Rando Sections (Modifier in place)	31
17. Dose Distribution with and without Beam Modification	32
18. Treatment Plan for Test of Computational Accuracy	34

Figure	Page
20. Calculated Dose Distribution along Tumor Plane	36
21. Comparison of Calculated and Measured Dose Distributions	37
22. Treatment Plan for Actual CT Outline of Rando Slice 14	39
23. Contours and Isodose Curves for CT of Slice 14	40
24. Calculated Dose Distribution Along Tumor Plane (Slice 14)	41
25. Comparison of Calculated and Measured Dose	42
26. Calculated Dose Distribution in Section 13	44
27. Calculated Dose Distribution in Section 14	45
28. Calculated Dose Distribution in Section 15	46
29. Measured Dose Distribution in Three Rando Sections (With and Without Beam Modification)	47
30. Contours and Isodose Curves for a Flat, Homogeneous Patient	53
31. Contours and Isodose Curves for a Homogeneous Patient with Actual Rando Phantom Surface	54
32. Calculated Dose Distribution at Midplane for a Flat Patient	55
33. Calculated Dose Distribution at Midplane for a Homogeneous Rando Phantom Section	56
34. Prescribed Dose Distribution	58
35. Unmodified Dose Distribution	59
36. Representative Tumor Points	59
37. Typical Irregular Field Treatment Area	63
38. TLD Calibration Curve	68

Figure	Page
39. Sample Treatment Plan for Computational Validation of Design	70
40. Contours and Isodose Curves for Section 13	71
41. Contours and Isodose Curves for Section 14	72
42. Contours and Isodose Curves for Section 15	73
43. Isometric Dose Profile for Section 13	74
44. Isometric Dose Profile for Section 14	75
45. Isometric Dose Profile for Section 15	76

Abstract

A method for designing radiation therapy beam modifiers is proposed. The design is based on a calculated dose distribution in the patient from an unmodified treatment beam. The modifier alters the beam before it reaches the patient in a way that yields the desired dose profile at the tumor. The design can be generalized to include any modifier material and any beam energy. The design was applied to an anthropomorphic phantom and verified using thermoluminescent dosimetry. The modifier was constructed of 1/2 inch square aluminum blocks. The dose distribution in the phantom, with and without beam modification, was measured. The modified dose profile approaches the desired distribution (maximum deviation of + or - 5%). Procedures for improving the results are suggested for further work.

Additional information is available in the report, AFIT/GEP/GNE/85M-10

BEAM MODIFICATION
FOR CANCER RADIATION THERAPY

I. Introduction

"The goal of radiation therapy is to achieve uncomplicated local-regional cure of cancer" (1:313). This is accomplished by delivering the prescribed dose to a tumor while minimizing the dose to healthy tissues. Several circumstances make this effort difficult at best, three of which are considered in this thesis.

One complication is the patient's irregular surface. A curved surface causes the radiation to pass through varying depths of tissue before reaching the tumor. This causes the beam to be attenuated more in the thicker regions. The result can be a non-uniform dose to the tumor.

Another complication is tissue inhomogeneity and the presence of voids. Khan indicates that, "In a patient, ... the beam may traverse layers of fat, bone, muscle, lung, and air. The presence of these inhomogeneities will produce changes in the dose distribution depending on the amount and type of material present..."(2:54).

The major complication is predicting the dose due to scattered radiation. The dose to a point in the patient can be conceptually divided into primary and scattered components. The primary dose results from interactions with unattenuated photons. The scattered dose results from Compton electrons and photons which have scattered to the dose point. Predicting this process is a significant problem in delivering the prescribed dose to the tumor.

Tissue Compensation

Much work has been done over the past decades in predicting the effects of these three complications on the dose distribution in the patient (2:Ch 10; 3:212-234). These calculational models were used in developing treatment planning that included these effects, but did not compensate for them.

At the same time, however, there were attempts to effectively eliminate the first complication with tissue compensation filters. First introduced by Ellis (4), tissue compensators are placed in the beam in order to make the patient's surface more closely resemble a plane orthogonal to the beam.

As shown in Fig. 1, the compensator is placed far enough away from the patient (15-20 cm) to remove the possibility of skin burns from the Compton electrons produced in the filter. Consequently, the lateral dimensions of the filter must be minimized because of the beam's divergence. The vertical dimensions of the filter are determined from the ratio of the attenuation factors of the compensating material and tissue.

Several methods for the design of tissue compensators have been proposed. A simple method uses metal wedges in the beam to approximate the shape of the tissue 'deficit' (5:18-20). Wedges, however, are generic devices and will not necessarily fit an individual patient.

Another method, described by Khan, "...uses thin rods duplicating the diverging rays of the therapy beam... The apparatus is positioned over the patient so that the lower ends of the rods touch the skin surface. When the rods are locked, the upper ends of the rods generate

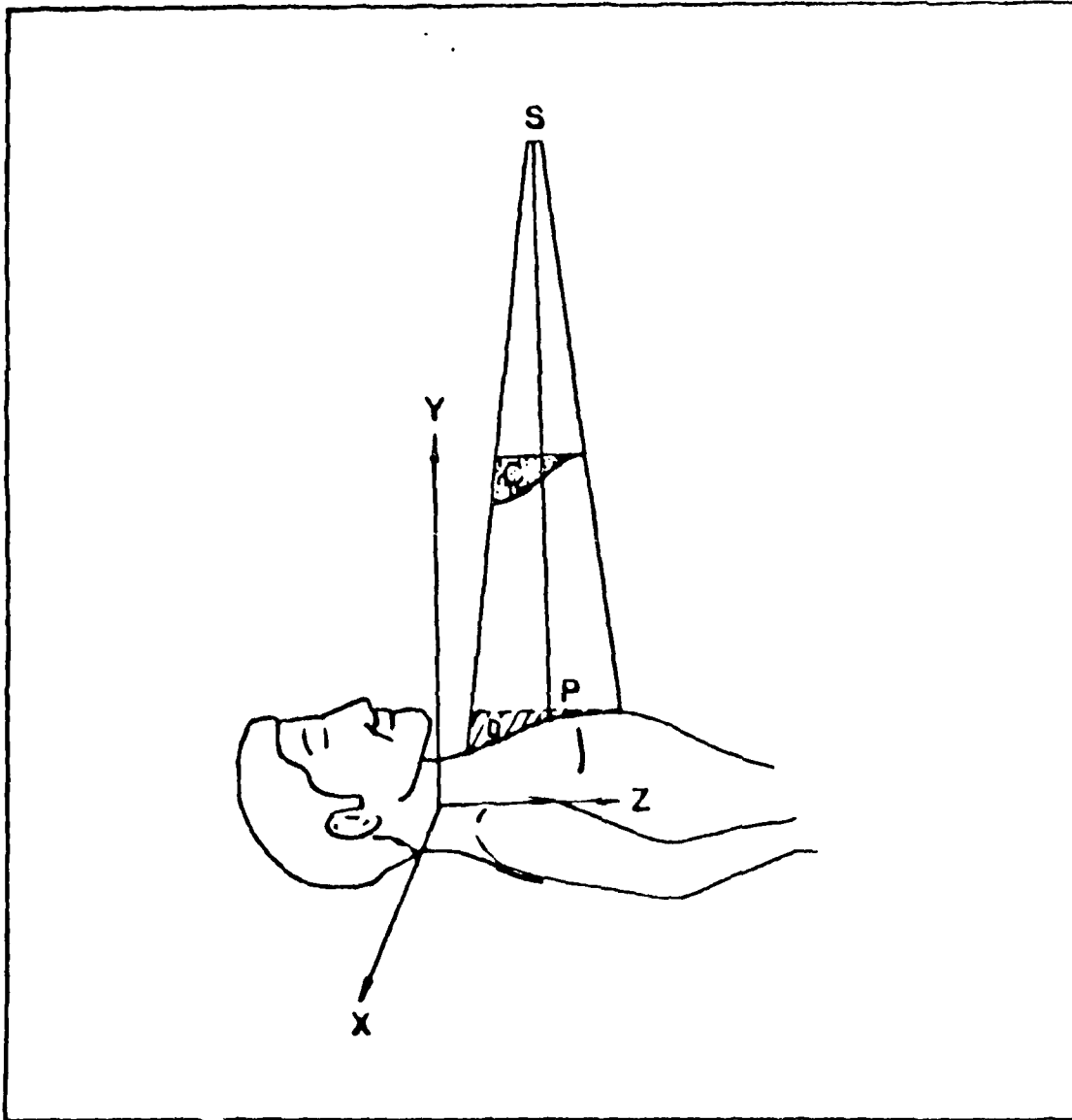


Figure 1. Placement of Compensator in Treatment Beam

P- Central Axis Point on Patient

C- Tissue Compensator

D- 'Tissue Deficit' being compensated for

S- Radiation Source

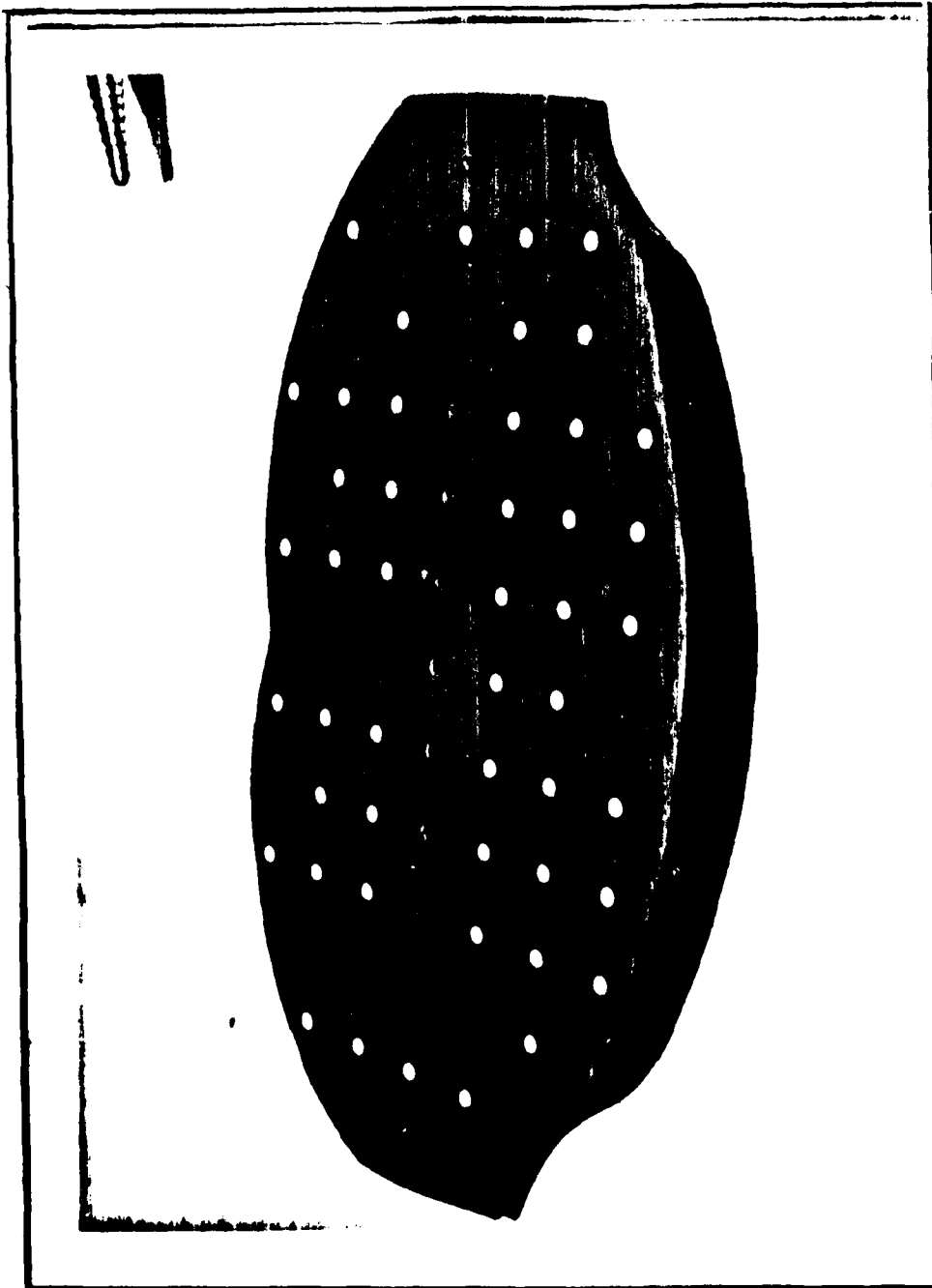


Fig. 7. Chest Section from the Rando Phantom

placement of TLD's (Thermoluminescent Dosimeters), to be used in dosimetry studies. A typical chest section of the phantom is shown in Fig. 7.

TLD's were used to measure the dose distribution in the phantom at selected locations. All the dosimeters were previously characterized statistically and calibrated to a known dose. The precision of the dosimetry was better than 3% at a 99% confidence level (Standard deviation $< 1\%$). A discussion of TLD theory and statistics is in Appendix D.

The source of the treatment beam in this work was Cobalt-60. An effective energy of 1.25 Mev for the gamma-ray beam was used. The treatment machine is shown in Fig. 8.

The modifier materials used in this research were aluminum blocks (1/2 inch square). The blocks were available in thicknesses ranging from 0.1 to 3.0 cm. The values of mass attenuation coefficient and density used in equation (2) were $0.055 \text{ cm}^2/\text{gm}$ and 2.7 gm/cc respectively. Being limited to a discontinuous modifier material posed some problems, but they were offset by the availability, simplicity, and re-usability of the aluminum blocks. A typical modifier is shown in Fig. 9.

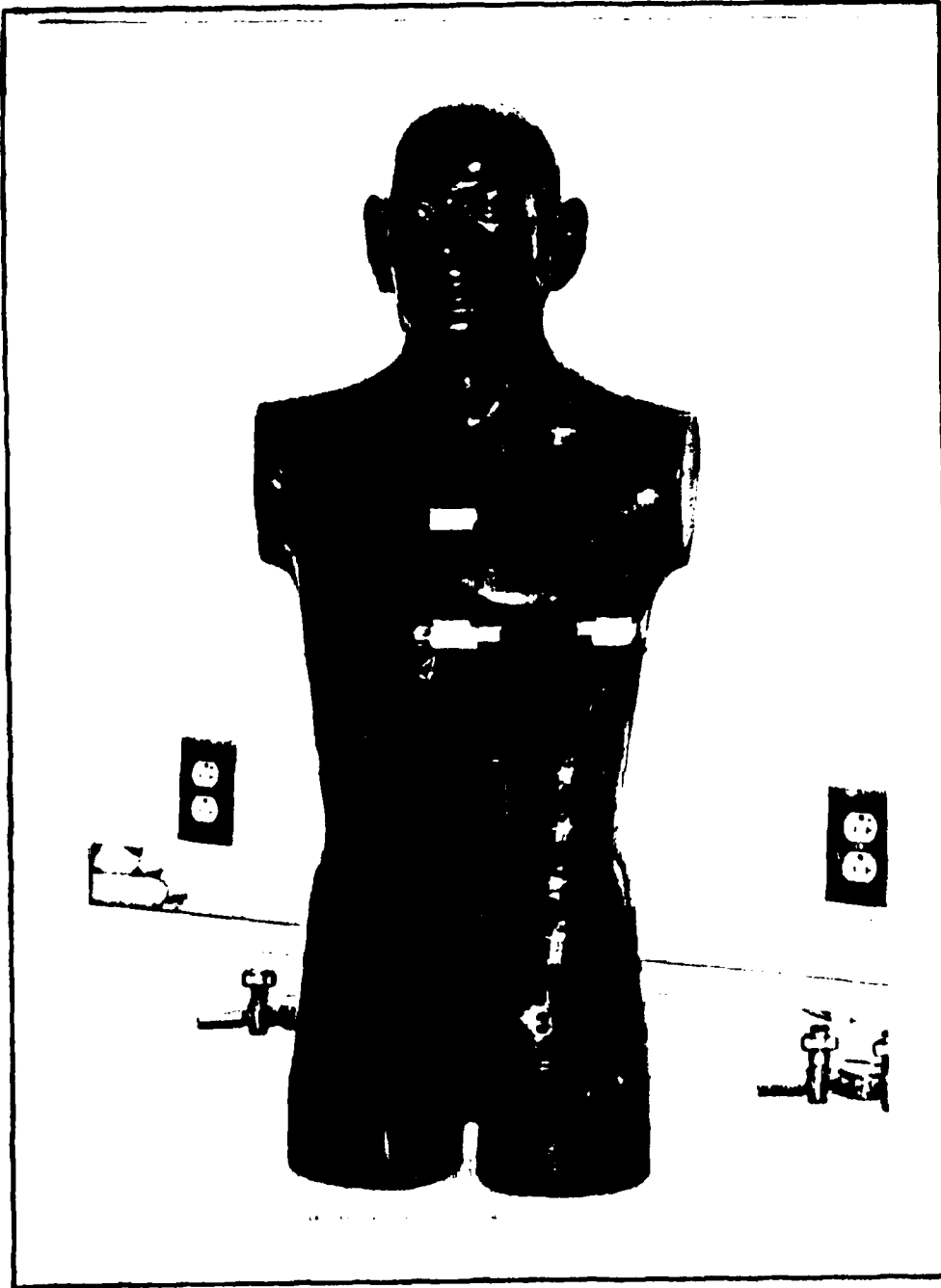


Fig. 6. The Alderson Rando Phantom

The use of this design method with irregular field and external beam treatment techniques needs investigation, although no major deficiencies are anticipated. The success of the method will depend on the availability of an unmodified dose distribution from a calculation. These two treatment plans are discussed in Appendix C.

This design can also be applied to a variety of treatment beam energies, provided the response of the modifier material to the radiation is known. Ideally, the beam would be mono-energetic and the modifier material would have a low scatter cross-section at that energy. Beams with an energy distribution could be applied by either assuming an effective energy or selecting a material with a relatively constant cross-section within the energy range. Otherwise, an energy dependent calculation would be required, causing the method to lose some of its simplicity.

Finally, most of the calculations required for this method can be programmed for automated design. The resulting dimensions of the modifier could be directly relayed to a numerically controlled router for automatic construction.

Validation Equipment

The modifier design was verified by using the Alderson Rando Phantom as a patient. The Rando phantom, shown in Fig. 6, is an actual human skeleton head and torso that incorporates tissue equivalent material throughout. The lungs are actual density and voids such as the trachea are included. It is sliced transversely in 25mm sections. Each section contains an array of holes for

Consequently, a lateral dimension of the modifier is minified by a factor of 0.727 in relation to its respective dimension at the tumor. This technique allows for beam divergence in a simple manner.

Discussion of Criteria

Conceptually, this modifier design shows the potential for satisfying several of the previously described criteria for an effective beam modifier. There is no need to consider the three major complications separately when the unmodified dose distribution is used as a starting point. The unmodified dose incorporates the combined effects of surface contours, internal inhomogeneities, and scatter. The modifier simultaneously accounts for all three effects and should deliver the desired dose distribution at the tumor.

Although, in the example cited, the prescribed distribution was a flat beam, the method could be generalized to any prescribed distribution. This generalization is discussed in Appendix B. In principle, the design would meet the first criteria: Delivering the prescribed dose. Attempts to verify this are discussed in section III.

The second criteria (use of CT scans) is an integral part of this method. In actual use, the unmodified dose distribution used as a starting point would be calculated using CT data.

This method can be used with any desired compensator material. Only the mass attenuation coefficient at the beam energy and the physical density of the modifier material are required for the calculation.

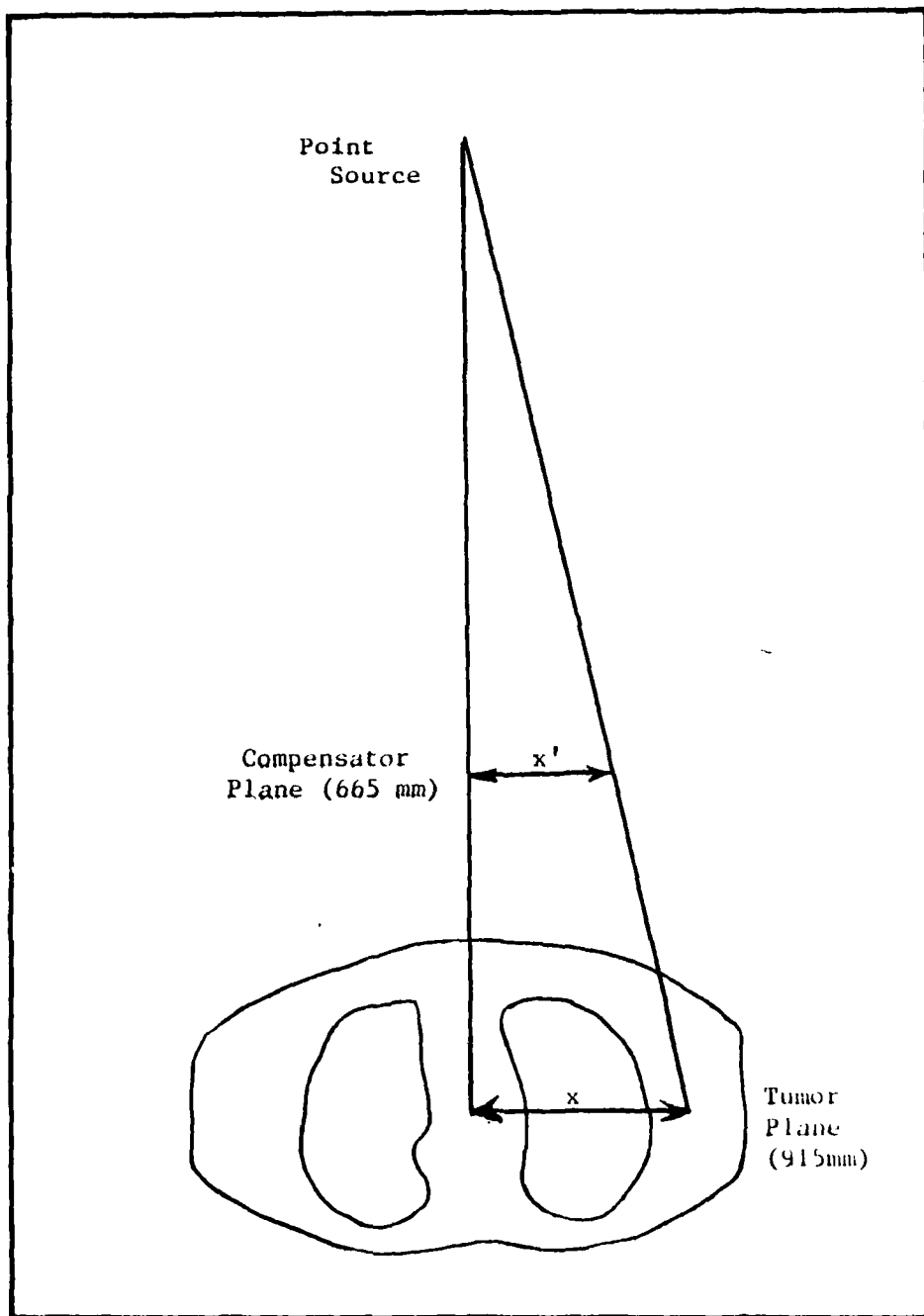


Fig. 5. Lateral Dimensions of the Modifier

The thickness of the modifier can now be computed, recalling that $n = 1$ at each point.

$$1/N_x = \exp(-u \cdot t_x)$$

Taking the logarithm of both sides,

$$\ln(1/N_x) = (-u \cdot t_x)$$

Dividing by $-u$, and including physical density, p ,

$$t_x = \frac{\ln(1) - \ln(N(x))}{(-u/p) \cdot p} = \frac{\ln(N(x))}{(u/p) \cdot p} \quad (2)$$

where (u/p) is the mass absorption coefficient. Thus the thickness of the modifier at each point can be determined from the unmodified, normalized dose and the properties of the modifier material.

Since the beam diverges, a point on the modifier will not be vertically above its corresponding point in the patient. The distance from a modifier point to the beam's central axis (x') can be determined from simple geometry, as seen in Fig. 5. The modifier dimension, x' , is related to the tumor dimension, x , by the respective vertical distances to the virtual point source of the beam. In this example, the modifier is 665mm from the source, the source-to-skin distance (SSD) is 800mm, and the tumor is 115mm deep in the patient. Thus the central axis distance to the source from the dose points is 915mm. Relating similar triangles,

$$\frac{665}{915} = \frac{x'}{x}$$

Solving for x' yields,

$$x' = 0.727 \cdot x \quad (3)$$

From these data, a dose distribution normalized to the minimum dose can be drawn. This distribution is shown in Fig. 4. The effect of the low density lung tissue on the distribution is apparent.

The prescribed dose distribution in this case will be a uniform dose along the tumor, with the dose at each point equal to the normalized value. The use of a normalized distribution allows relative changes to be made. If the absolute dose is different, the exposure time can be varied accordingly, still maintaining the shape of the normalized distribution. It is the job of the beam modifier, in this case, to alter the beam before it reaches the patient in a way that yields a flat dose distribution at the tumor.

The problem reduces to one of determining how much attenuation the beam needs above each data point in order to reduce the dose at that location to the minimum value (132 rad in this case). All the values that are presently greater than 1 in the normalized distribution should be reduced until they equal 1. We define...

n = desired normalized dose at the point (1 in this case)

N_x = existing normalized dose at the location x (Fig 4).

To reduce N_x to the value of n , the amount of attenuating material required is calculated from the following relationship,

$$n = N_x * \exp(-u*t_x) \quad (1)$$

where

u = the absorption cross section for the modifier material
at the beam energy

t_x = the thickness of the modifier at location x .

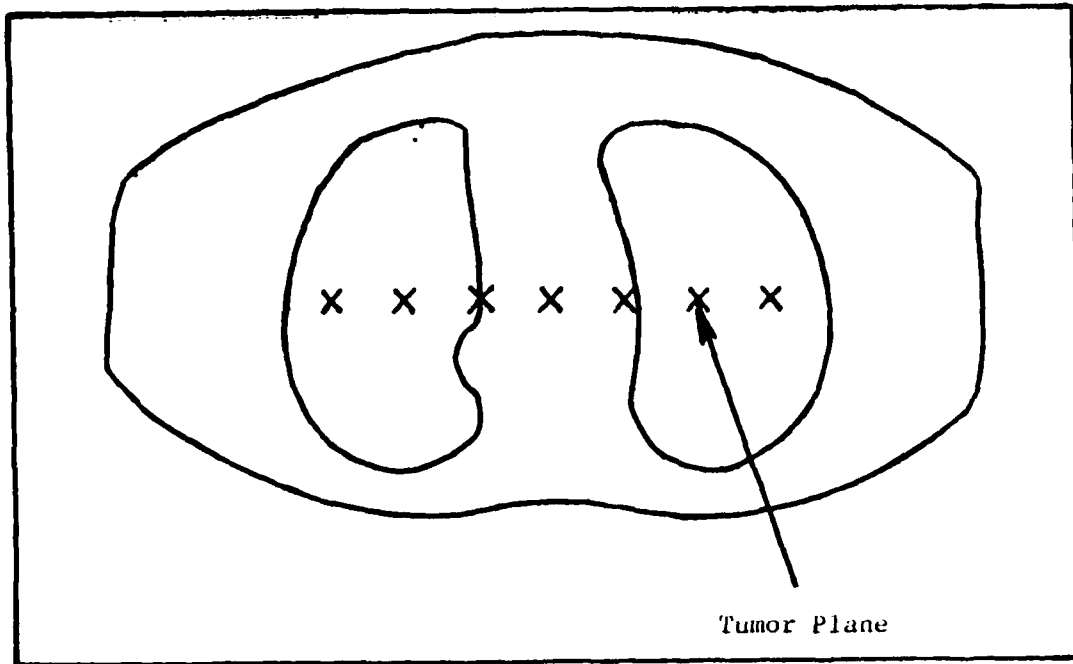


Fig. 3. Typical CT Scan Slice

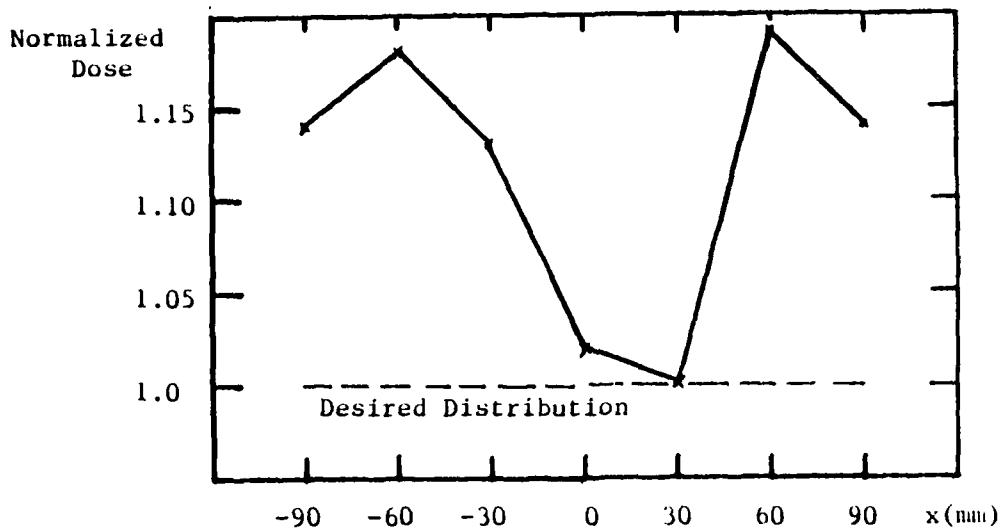


Fig. 4. Normalized Dose Distribution at Tumor Plane

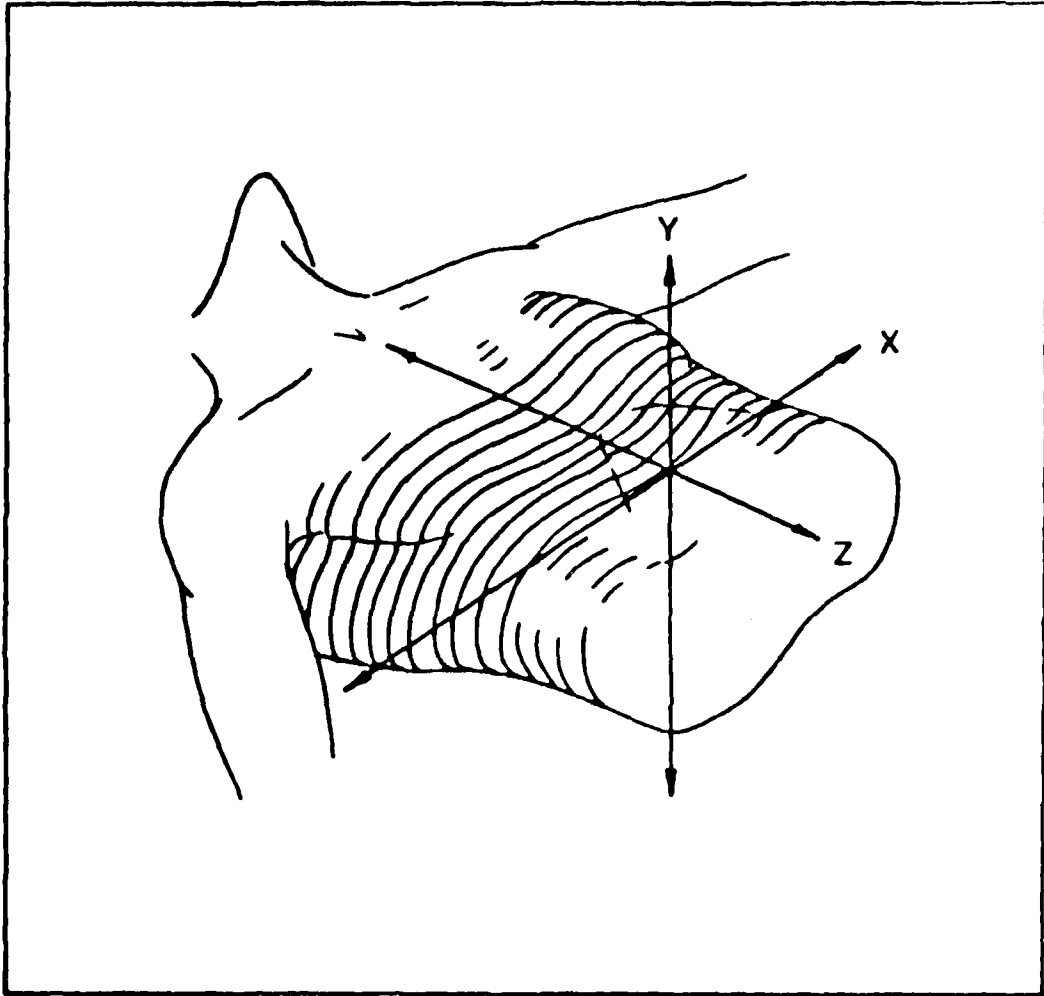


Fig. 2. Co-ordinate System with respect to Patient Orientation

II. Design Methodology

The design for the beam modifier starts with the dose distribution in the patient resulting from exposure to an unmodified beam. This dose distribution can be calculated or measured empirically. How it is measured or calculated will be discussed in section III. For the purpose of illustration, it will be assumed that an unmodified dose distribution is available and correct.

Derivation

The co-ordinate system to be used throughout this thesis is shown in Fig. 2. An outline of a typical CT scan slice, with tumor locations marked, is shown in Fig. 3. For demonstration of the method, it is assumed the tumor location is a horizontal line at $Y=0$. The dose along the tumor is known at the points indicated for exposure to the unmodified beam. Table I shows the dose at each data point.

x (mm)	-90	-60	-30	0	30	60	90
Dose (rad)	151	156	149	134	132	157	150

Table I. Dose at Selected Locations

Design Method Outline

The product of this research is a method for designing beam modifiers based upon a calculated dose distribution in the patient from an unmodified beam. The calculations are performed by the RTP (Radiotherapy Treatment Planning) software provided by CMS, Inc. (Computerized Medical Systems, St. Louis , MO).

CT scans of the patient are entered into the computer. The surface contours and important internal features are outlined by the computer and the physical densities of the features are entered. The program then calculates the dose throughout each slice from an unmodified treatment beam. The dose distribution is normalized to the minimum dose in the field. This distribution is then compared to the prescribed dose distribution (eg.- a flat, uniform dose at tumor depth). The thickness of the modifier at each point is calculated by determining how much attenuation is needed to reduce the unmodified dose at the point to the prescribed dose. The beam is assumed to be attenuated exponentially through the modifier. The lateral dimensions of the modifier are determined from the beam divergence.

for correcting for 'missing tissue', we might think of it as a means to modify the external radiation fields so as to achieve a desired dose distribution within the patient" (9:483).

Ellis devised an early method for combining compensation for contours and density differences (10). More recent clinical methods use exit dose information from the patient for designing the modifier (11). The exit dose is recorded by film placed under the patient during treatment. A computerized dosimetry system then reads the film and generates dose information.

Modifiers designed from exit dose information are an improvement over earlier methods. However, they still may not deliver the desired dose distribution at the tumor. The modified beam will be uniform only at the exit plane, not necessarily where uniformity is desired.

Problem Definition

The purpose of this enterprise was to improve on earlier methods and develop a simple design for beam modifiers. The design would ideally meet the following criteria:

1. Deliver the desired dose distribution in the patient
2. Use the information available in CT scans
3. Adapt easily to different modifier materials
4. Could be applied to both external beam and irregular field treatment plans (Discussed in App. C)
5. Could be used for a variety of beam energies
6. Could eventually be constructed automatically for clinical use

The relative importance of these criteria, and their application to the proposed method, will be discussed later in the thesis.

a surface similar to the skin surface, but corrected for divergence. A plastic compensator can then be built over this surface"(2:262).

One method involves moving a pivoted pointer, connected to a router, over the patient's surface (6). Still another method uses photogrammetry, "...the technique of making geometric measurements from a photograph" (7:505).

Recently compensators have been designed from the very accurate contour information available in CT (Computed Tomography) scans. The advantages of this method include better reliability, more accuracy, and less patient discomfort. In 1982, Higgins developed computer software that designs tissue compensators from CT input (8).

All of the above methods do compensate for surface irregularities, but the resulting dose distribution can still deviate from that prescribed because of the other effects (ie.-inhomogeneities and scatter). Tissue compensation, therefore, is a necessary but generally not sufficient technique for delivering the prescribed dose.

Indeed, a tissue compensator can sometimes cause the dose distribution to become less uniform. It does so by cancelling out the inherent 'beam-flattening' shape of the patient (convex-upward). This situation is discussed in Appendix A.

Beam Modification

To be of general usefulness, a beam filter must simultaneously compensate for surface irregularities, density differences, and scatter. Renner suggests, "...it would seem appropriate to enlarge our definition of the tissue compensator. Rather than merely a device

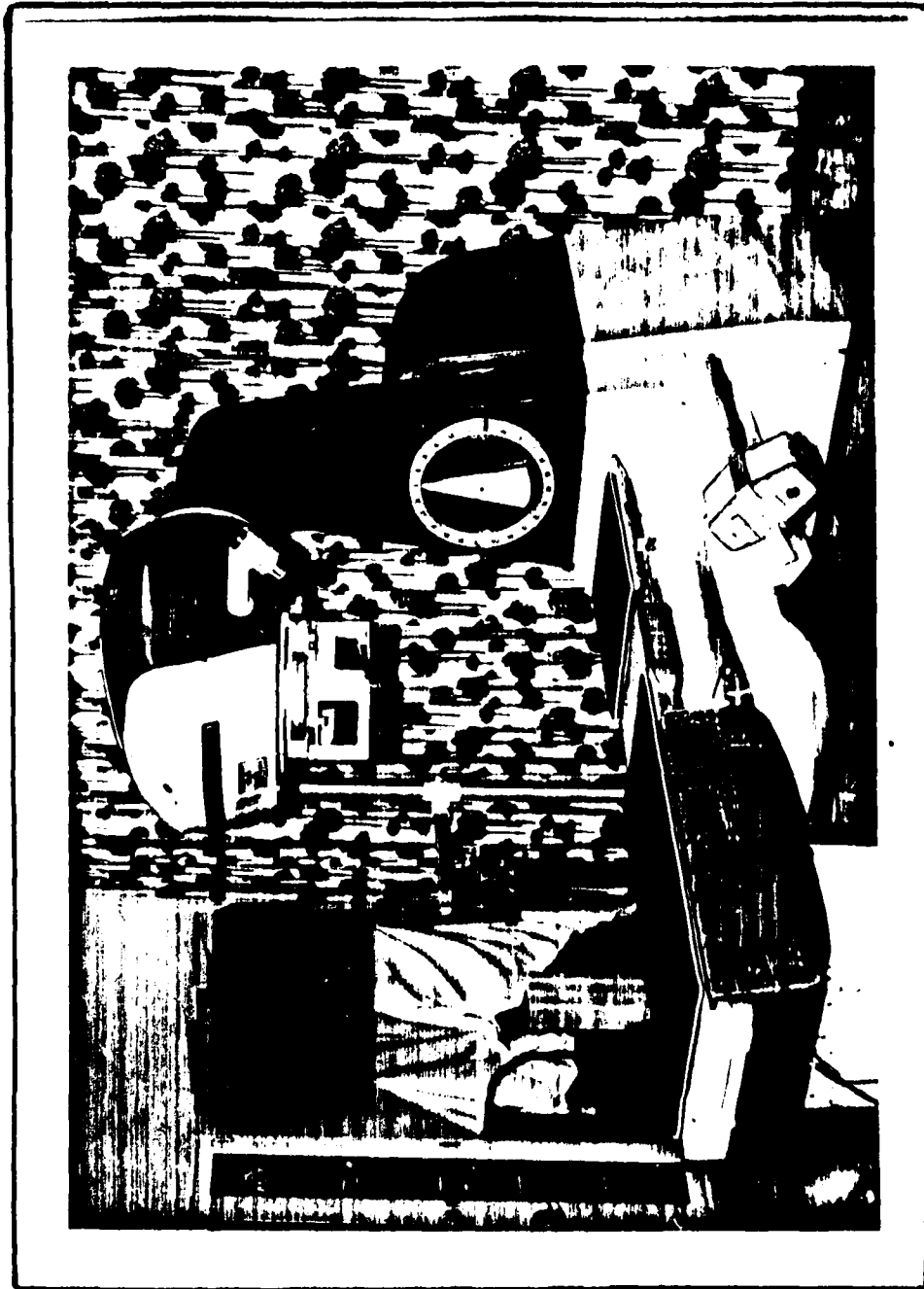


Fig. 8. The Cobalt-60 Treatment Machine

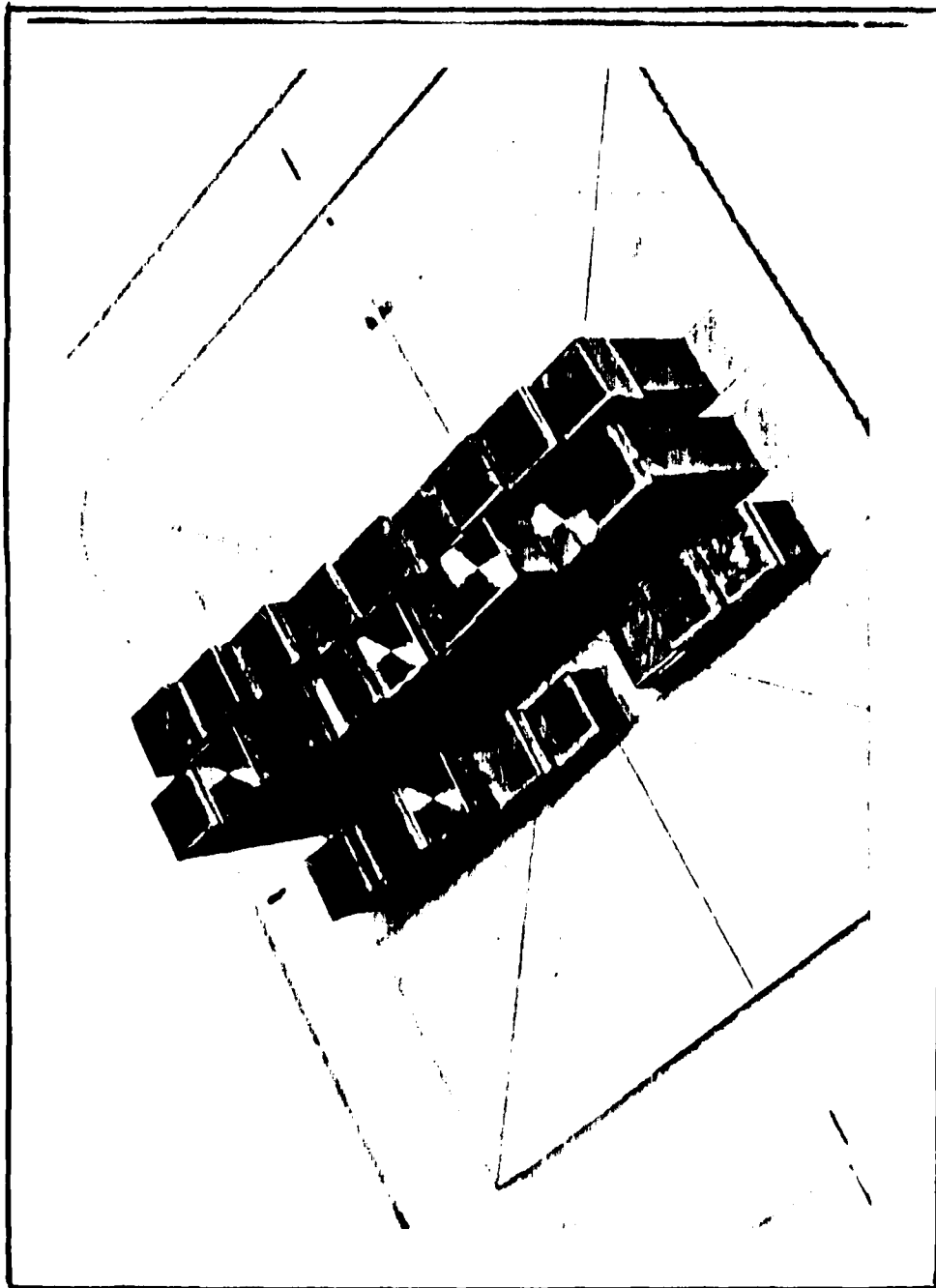


Fig. 9. An Aluminum Block Beam Modifier

III. Results

Preliminary Tests

Tissue Compensator Test The first dosimetry test involved the use of a tissue compensator designed by Higgins for the Rando phantom (8). Exposing the phantom to the beam with and without the compensator in place gives an indication of its effectiveness.

TLD's were placed in a coronal (x-z) plane in eight chest sections numbered 11 thru 18. The normalized dose distribution from the unmodified beam is shown for each slice in Fig. 10. The compensator was then placed in the beam and the dose recorded (Fig 11).

The beam did flatten somewhat in places where the phantom was relatively homogeneous. But the effect of density differences was so pronounced that it became obvious that tissue compensation is not sufficient to deliver a uniform dose. This again leads to the conclusion that actual beam modification should be the goal.

Scatter Determination Test Another experiment was performed to determine the effect of scatter on the dose distribution. This effect was previously mentioned as the third complication in delivering a uniform dose. It should be recognized that the other two complications (surface contour and density differences) are constant for a patient. Scatter, however, depends on the amount of primary radiation reaching the patient. Therefore the introduction of a modifier into the beam will reduce the scatter, perhaps in an adverse way.

Normalized Dose
(Repeated
Scale)

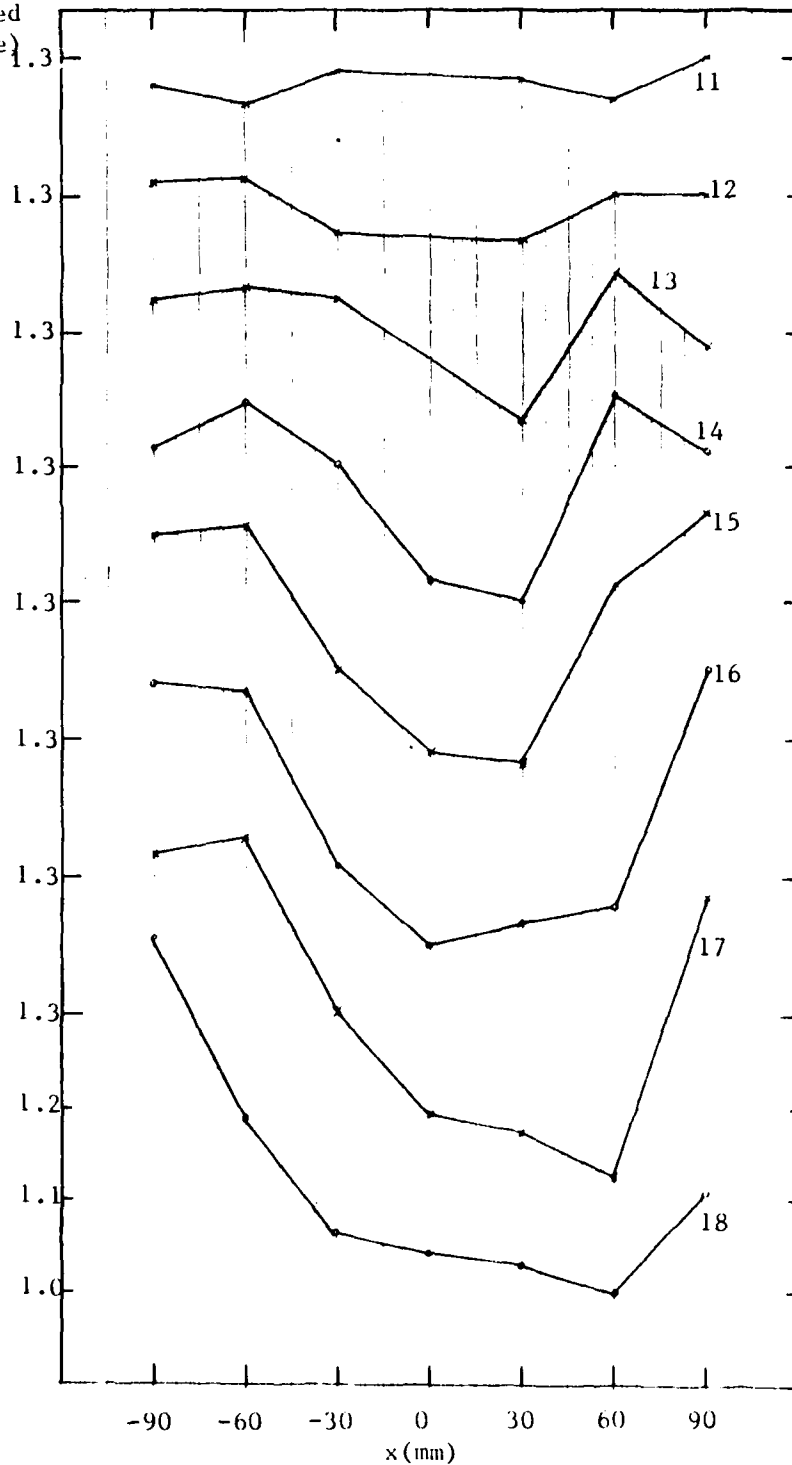


Fig. 10. Dose Distribution in Rando Sections
11-18 from an unmodified beam

Normalized Dose
(Repeated
Scale)

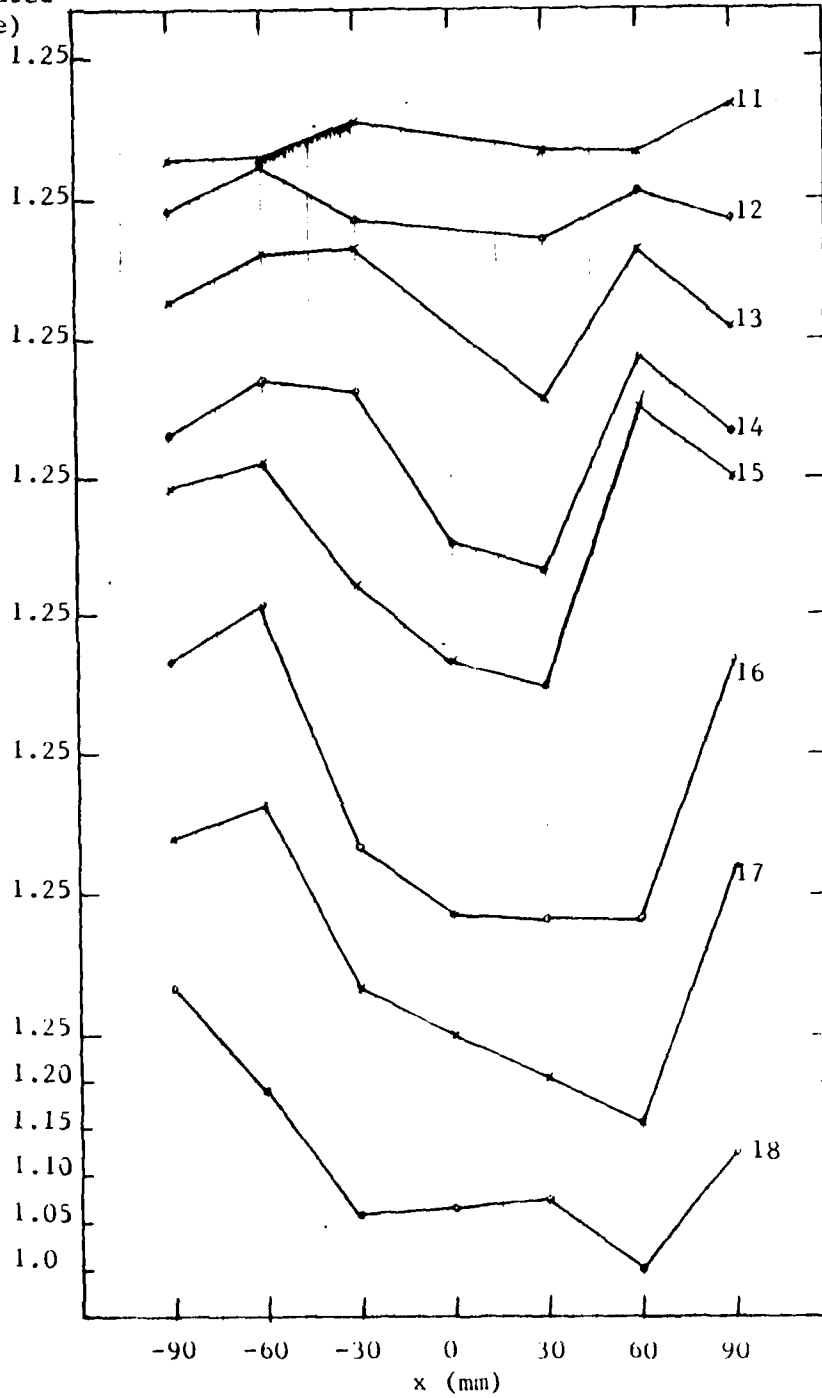


Fig. 11. Dose Distribution in Rando sections 11-18 from a beam with Higgins' tissue compensator in place

If the modifier abruptly changes the scatter contribution to the dose, then an iterative design process would be needed. Before this can be determined, a qualitative understanding of the scatter contribution to the dose is needed. This information was obtained by measuring the dose to a chest section of the phantom exposed in three different media. In each case, the TLD's were placed in a horizontal line at $Y=0$. Also, each time the section was placed vertically at the beam center. The beam size was 25x25 cm at 80cm SSD.

The first measurement was taken with the section in air. This gives a dose distribution with minimal scatter. The second measurement was taken with the section suspended in water. An increase in dose over that in air is expected, due to the scattered radiation from the more dense material around the section. The third measurement was taken with the section in the Rando phantom itself. An increase in dose over that in air results from the scatter from adjacent sections of the phantom.

The dose distribution for each measurement is shown in Fig. 12. The dose in the phantom is less than that in water. This is because the adjacent lung tissue, being less dense than water (0.3 gm/cc vs. 1.0 gm/cc), is less effective at scattering into the section of interest. As expected, the dose in air is less than the other two.

More importantly, it can be seen that the relative shape of each distribution is quite similar to the others. Since the only difference is the amount of scatter, we can conclude that the shape of the dose distribution is determined from the primary beam. The scatter contributes by increasing the absolute dose in the distribution.

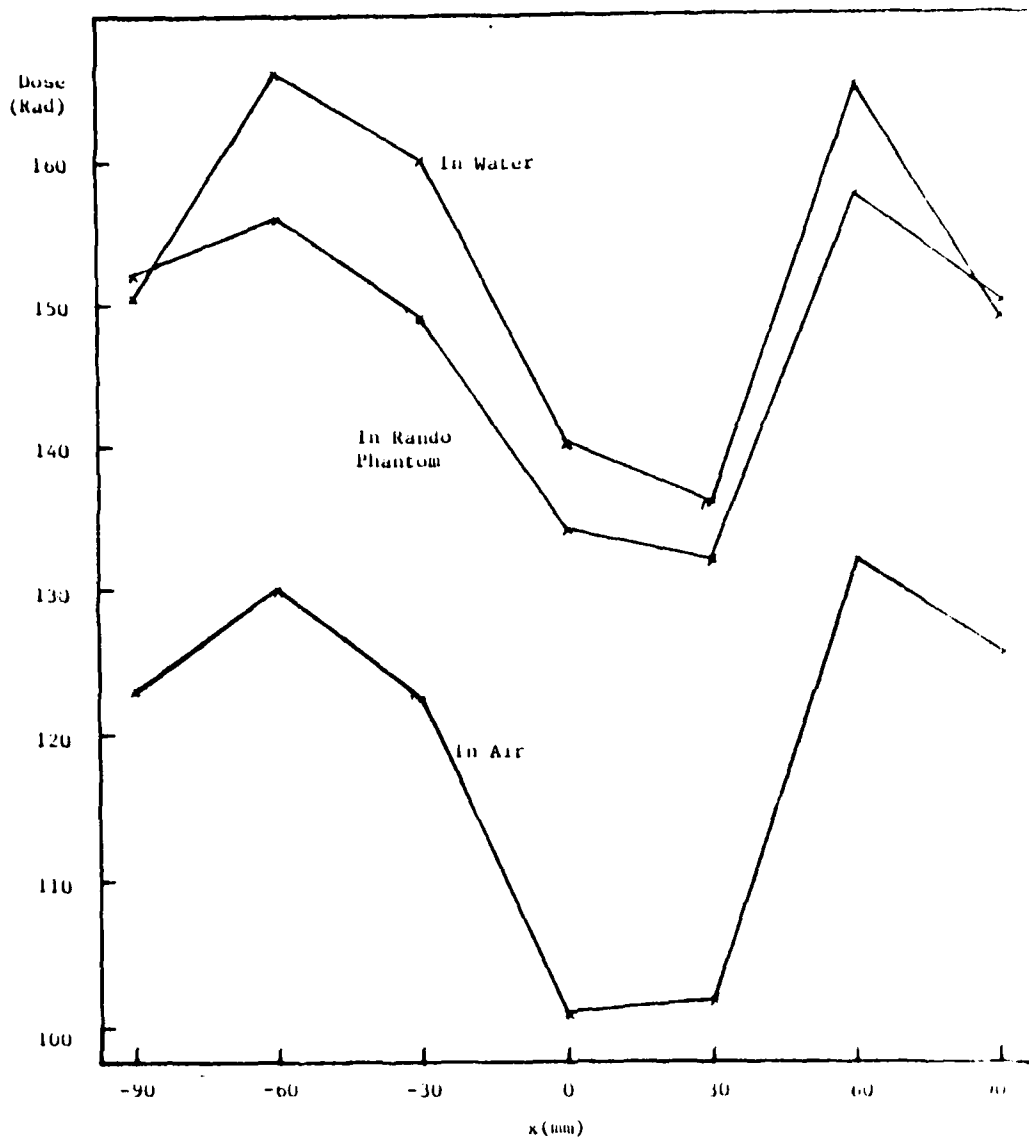


Fig. 12. Dose Distribution in Rando Section 14
in Three Media

The scatter contribution to the dose profile can be thought of as a 'tide' that raises the level of the distribution. This means that the modifier design is still sound. Because the primary beam is shaped to the prescribed distribution by the modifier, the resulting dose (which includes primary & scatter) should maintain the prescribed distribution. The scatter will affect the absolute level of the distribution, but not alter its shape dramatically. That is the function of the beam modifier: to maintain the correct relative shape of the dose distribution. The absolute level can be corrected by simply changing the time of exposure to the beam.

This treatment of scatter, however, is only an approximation. The impact of scatter at various depths was not investigated. Also, the nearby presence of bones can affect the scatter contribution locally. Although, in this research, scatter is regarded as a minor contributor to relative dose profile, future efforts should not be limited by this assumption.

Design Verification

Validation of Empirical Design The first test of the modifier design used the actual measured dose distribution in the phantom as a starting point. This dose in three Rando chest sections from a narrow, unmodified, anterior beam were recorded as a function of x at $Y=0$. The resulting normalized dose distribution is shown in Fig. 13. A narrow beam (25x8cm at 80cm SSD), encompassing only three sections, was used to decrease the turnaround time between the testing of various modifier designs (since beam size determines modifier size).

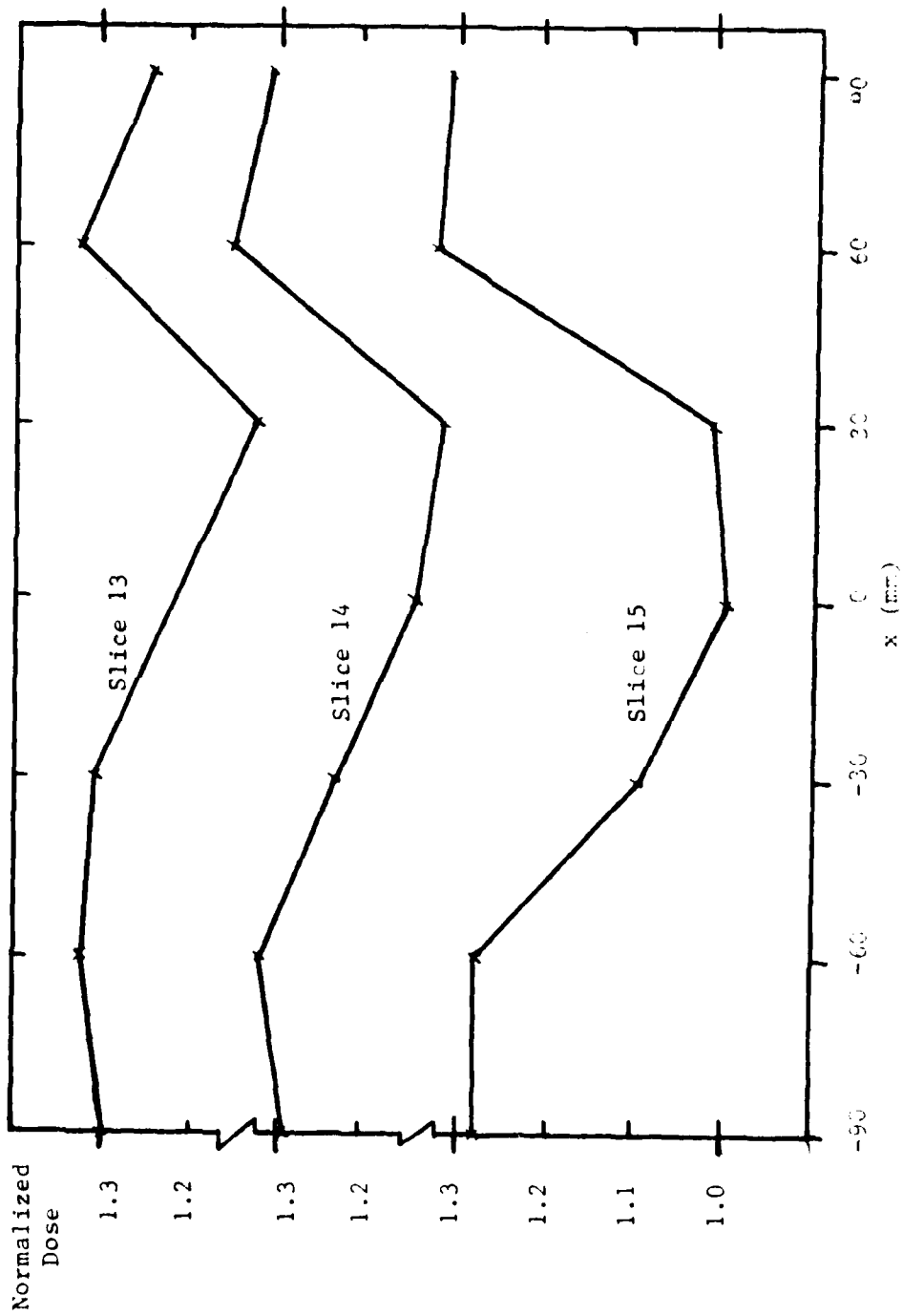


Fig. 13. Normalized Dose Distribution for Inree Kando Sections (Unmodified Anterior Beam)

The normalized dose in Fig. 13 was used in equation (2) to calculate the thickness of aluminum needed to flatten the beam at the TLD (tumor) plane. Of course, in a real patient, such a-priori empirical dose information is not available and must be calculated. The purpose of this test was to determine whether the method could work at all. Given the actual dose from an unmodified beam, the prescribed distribution (flat and uniform in this case) should result. If the method is not successful given this information, then it could never work. But if it is successful, then the problem reduces to getting calculated dose distributions that reflect the actual situation.

A modifier was thus designed and constructed. Because the dosimeters were 25mm apart (section thickness), data were only available at this spacing in the z-direction. The corresponding lateral distance at the modifier is 18.2mm. Since the aluminum blocks are available only with 1/2 inch lateral dimensions (12.7mm), they could not be placed side-by-side and still be over the correct location in the patient. This results in a 5.5mm gap between the rows of aluminum blocks for each section. This situation is shown in Fig. 14.

The gaps between the rows of modifier allows some unwanted primary beam to reach the patient. Nonetheless, it was concluded that, in the interest of time, that effect could be tolerated. This problem could be eliminated by having data in the z-direction at 17.5mm intervals rather than 25mm (easily done with CT). This would allow the rows of modifier blocks to be adjacent. Also, a continuous modifier material could be used.

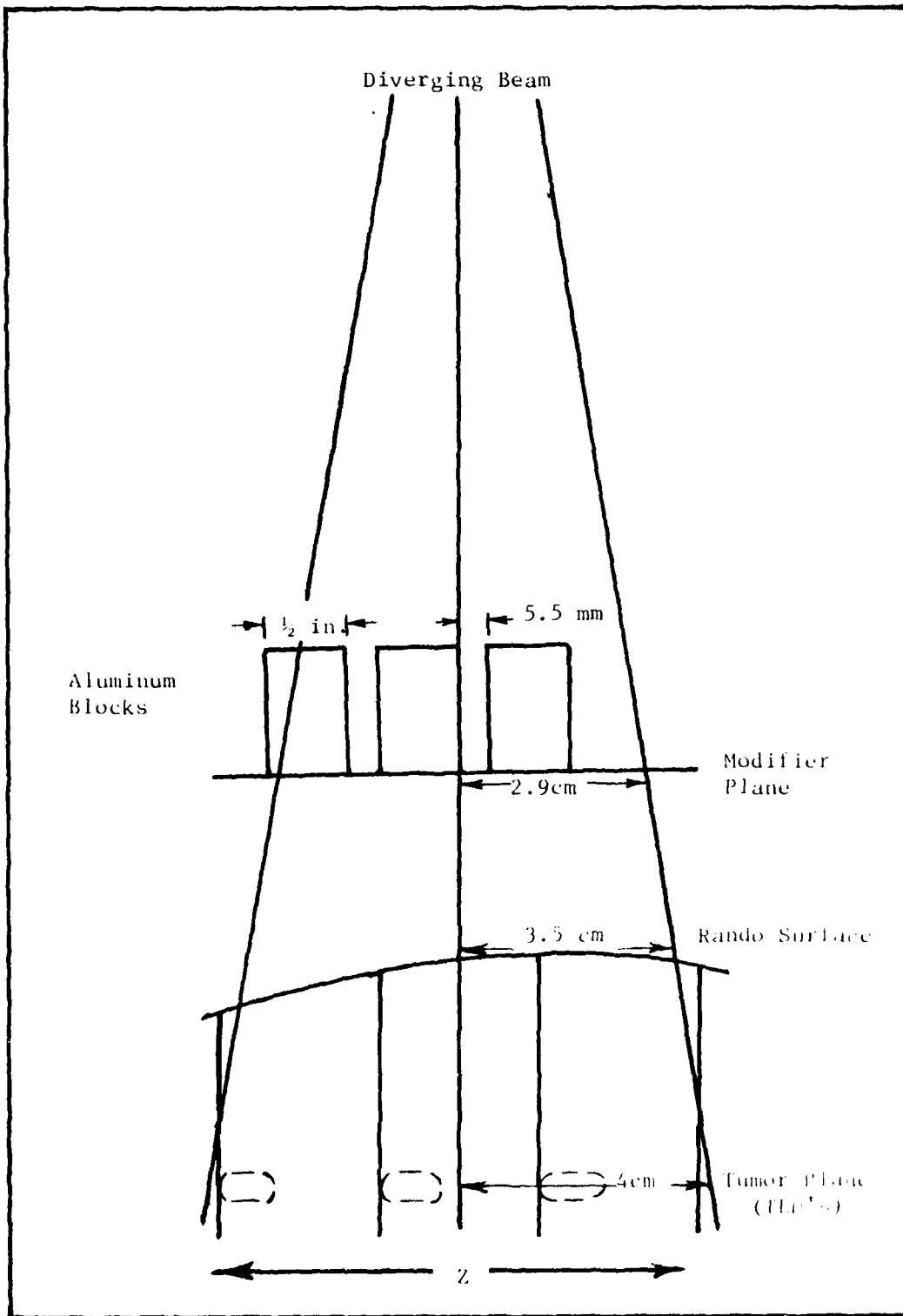


Fig. 14. Geometry for Modifier in z-direction

The phantom was then exposed with the modifier placed in the beam. The beam was centered as before, and was set at a 25x8cm field size. The TLD's were placed in the same locations. The resulting dose distribution for the three sections is shown in Fig. 15. The dose in each slice varies from a flat distribution by less than 10%. The variation from uniformity can be partially explained by the additional primary beam penetrating through the gaps in the modifier. If a continuous modifier were used, even better results could be expected.

A second exposure was made with the beam's central axis over the TLD's rather than centered over the middle section (5mm along z axis). The resulting distribution is shown in Fig. 16. Again, the profiles are within 10% of the prescribed uniform dose.

From these results, it can be concluded that the modifier design does deliver (within 10%) the prescribed dose distribution. For comparison, Fig. 17 shows the dose distribution with and without the modifier in place. While the results are acceptable, improvement is expected when the gaps in the present construct are removed.

Since the success of the modifier is predicated on knowledge about the unmodified dose distribution, it is essential that any calculational source of that distribution reflect reality. The next section investigates that issue.

Validation of Calculational Design Having determined that the design method is successful in modifying the dose distribution, the next step was to extend the method by using calculated dose profiles as a starting point. This is necessary because a measured dose

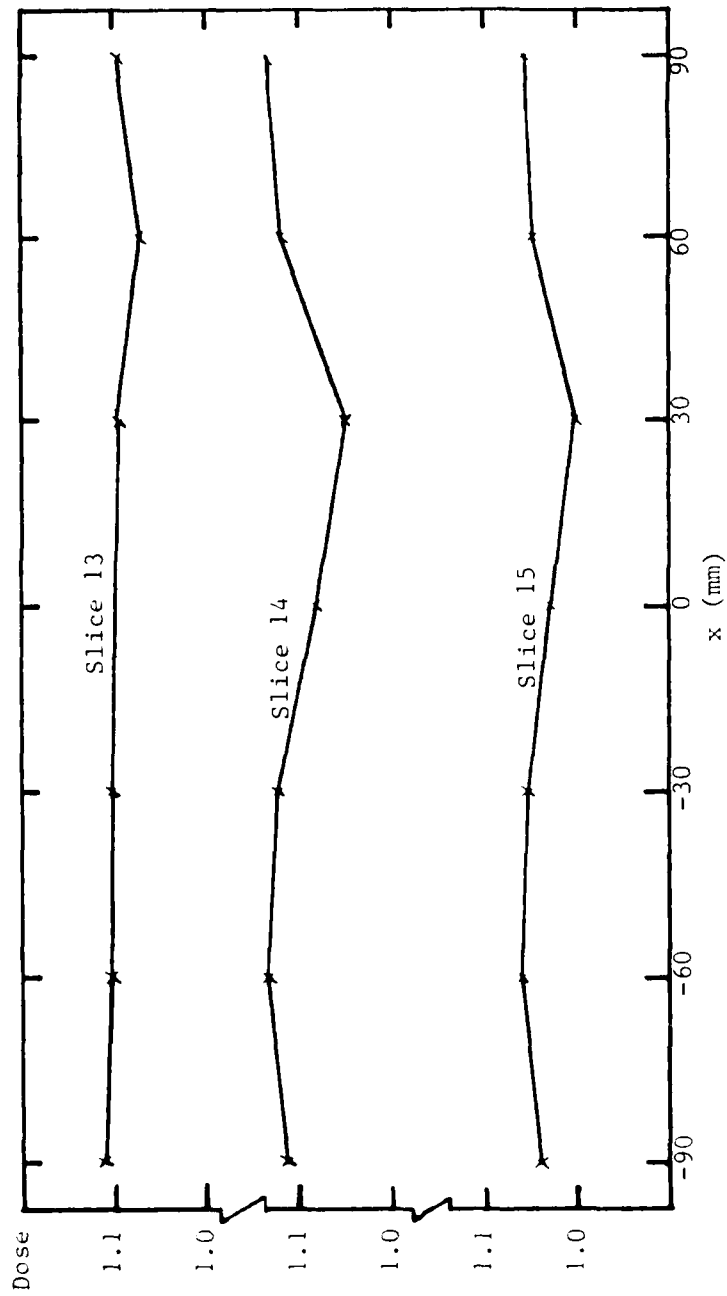


Fig. 15. Normalized Dose Distribution in Three Rando Sections
(Modifier in place)

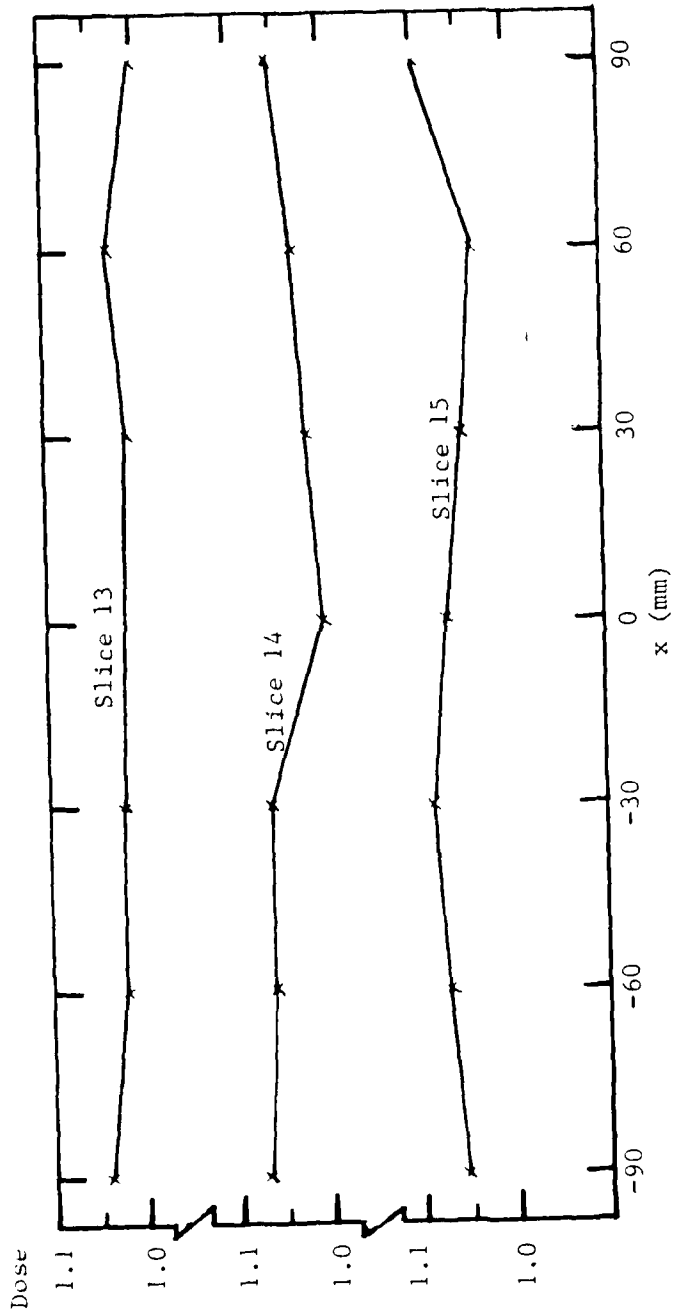


Fig. 16. Normalized Dose Distribution in Three Rando Section
(Modified Anterior Beam)

OSE (Rad)

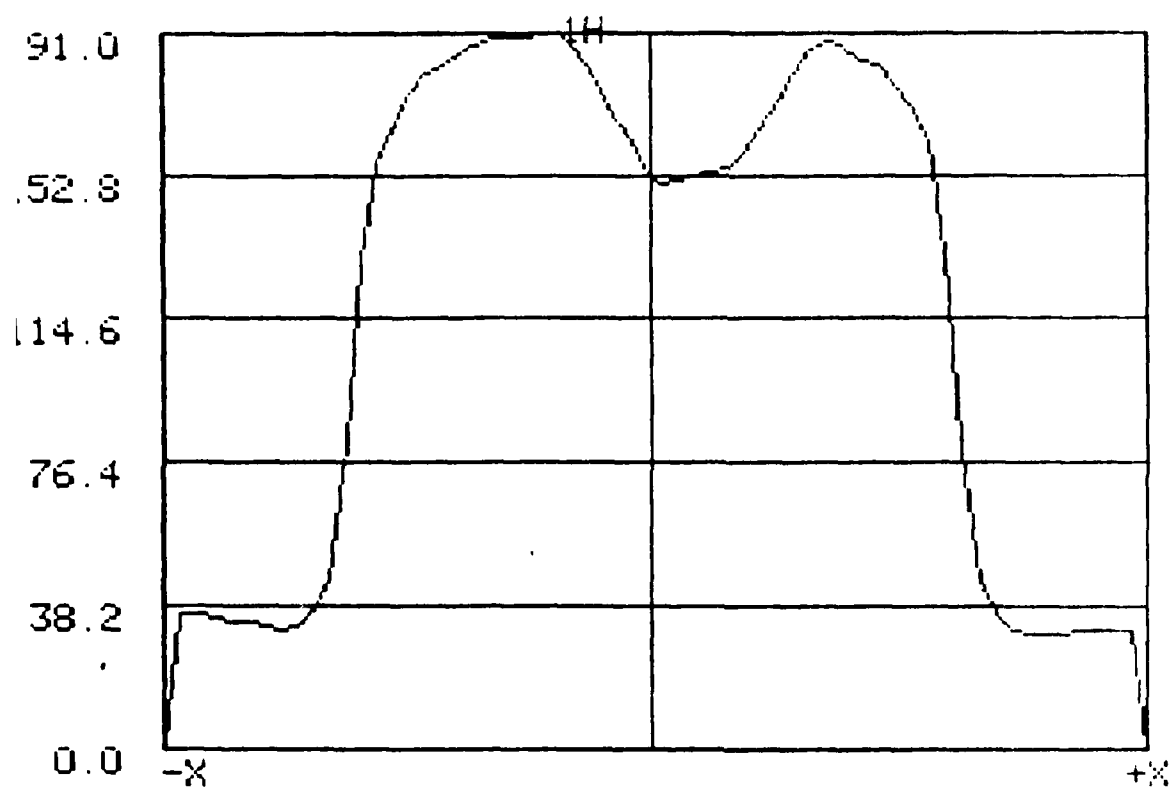


Fig. 27. Calculated Dose Distribution in Section 1.

DSE (Rad)

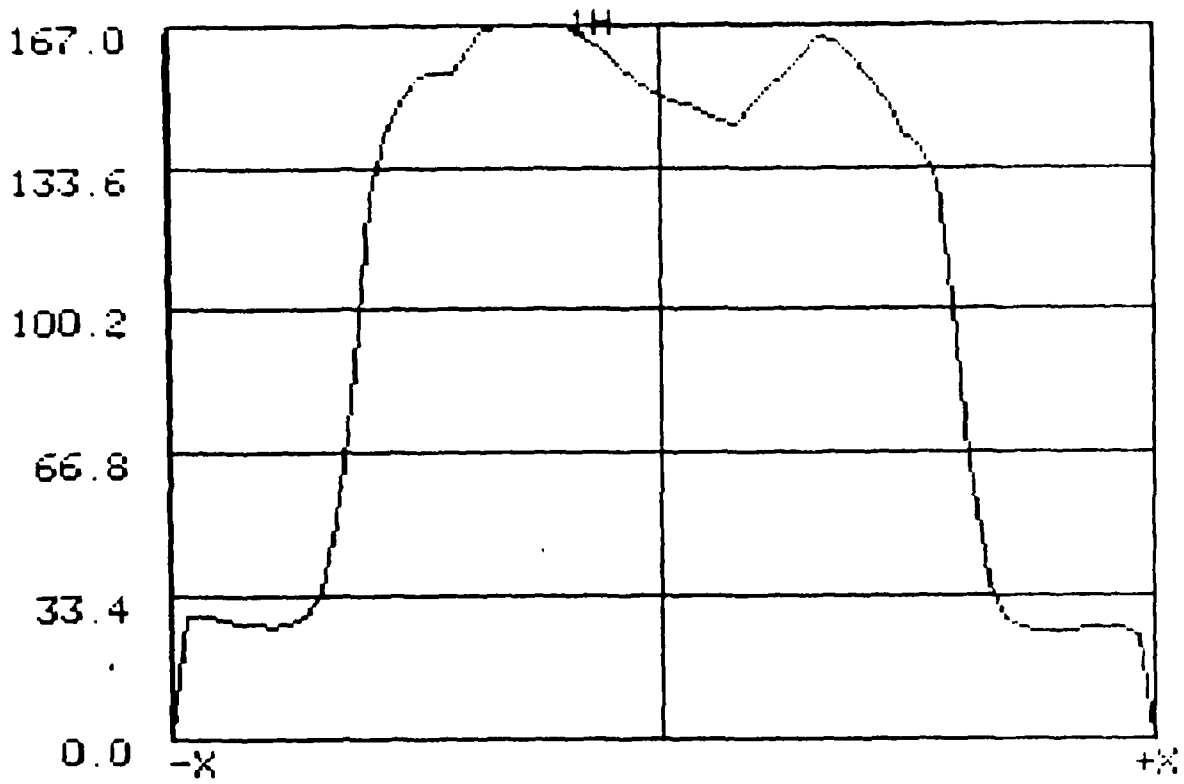


Fig. 26 Calculated Dose Distribution in Section 13

definition of contours and density, the programming does compute dose distributions that approximate reality. Whether those calculated distributions would be suitable for the design of working modifiers was determined next.

Again, to decrease turnaround time between tests, modifiers were designed for a narrow treatment beam (25x8cm at 80cm SSD). The same three sections of the phantom (#13,14,15) were used. Dosimetry in these slices from an unmodified anterior beam is available in Fig. 13. Similar dose information was calculated by the computer. A modifier was designed from the calculated distribution by using equation (2) and by accounting for beam divergence. The phantom was exposed to the same beam with the modifier in place and the dose was measured.

The contours and tissue densities were entered for all three slices on the CT scans. The treatment beam was then defined. The dose in each slice was calculated independently. The resulting dose distributions at the tumor plane are shown in Figs. 26-28. The iso-dose curves for each slice is shown in Appendix E, along with the corresponding treatment plan and 3-D dose profiles. Information was obtained from these profiles at intervals that correspond to the aluminum block spacing of the modifier. This information was used in equation (2) for the design and construction of a modifier that would deliver a uniform dose at $Y=0$.

The phantom was exposed to the narrow beam with the new modifier in place. The resulting dose distribution was measured with TLD's. It is shown in Fig. 29, along with the profile from the unmodified

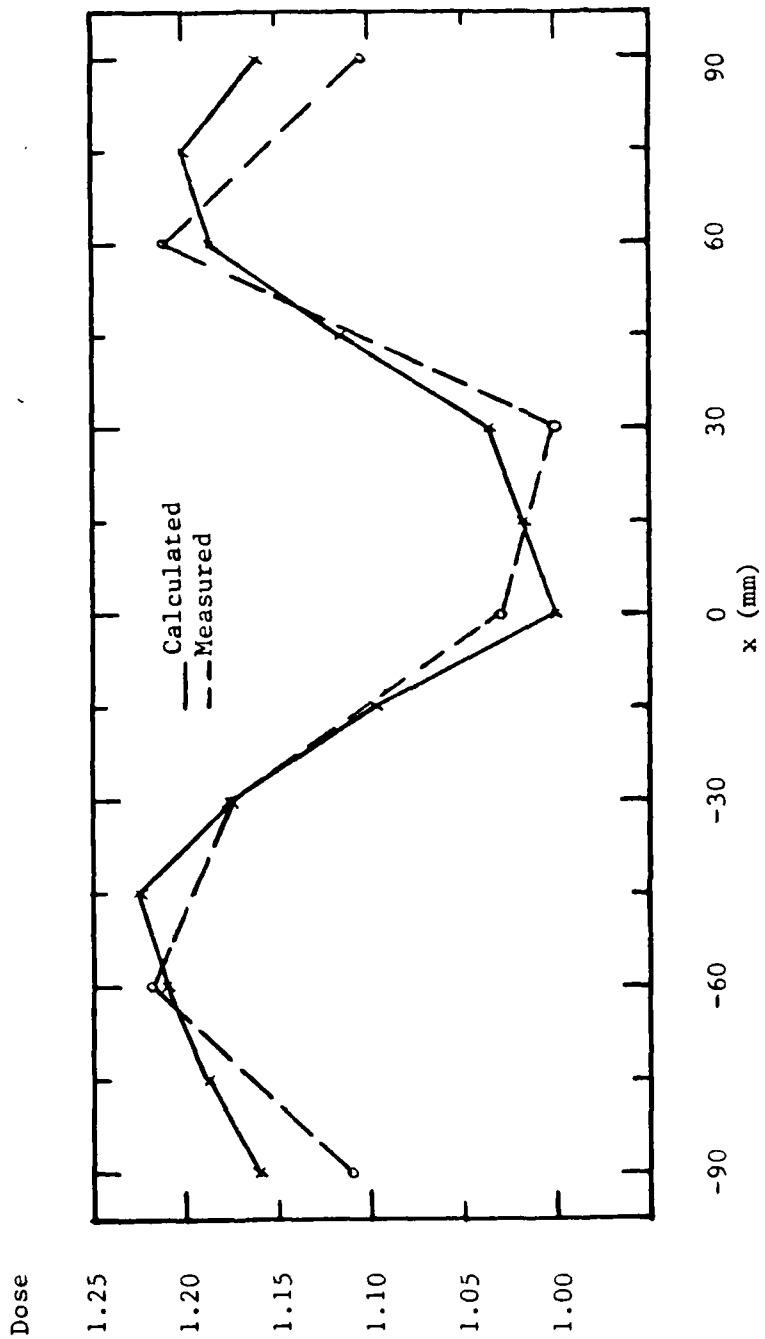


Fig. 25. Comparison of Calculated and Measured Dose Distributions

DOSE (Rad)

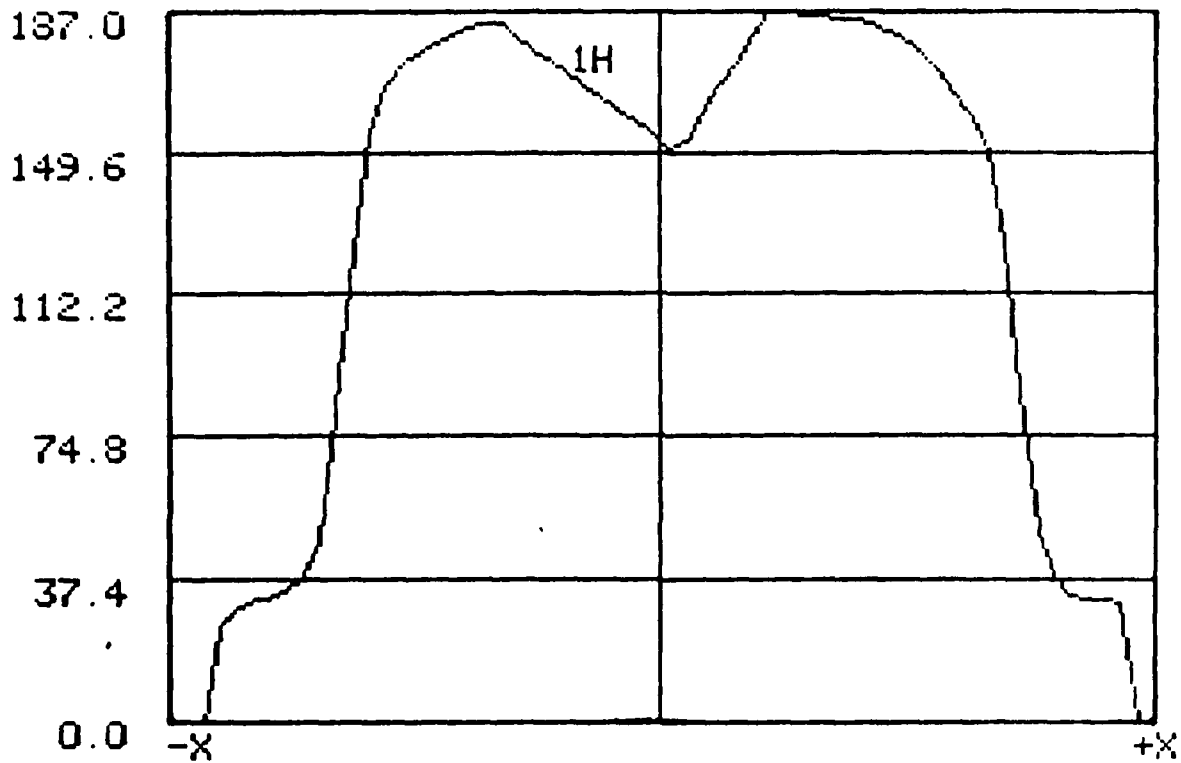


Fig. 24. Calculated Dose Distribution Along Tumor Plane for CT scan

ISODOSE	0	1	2	3	4
VALUES	200	175	150	125	100

CONTOUR	DESCRIPTION	DENSITY GM/CC
A PATIENT	SURFACE	1.00
B INTERNAL	L LUNG	.30
C INTERNAL	R LUNG	.30
D INTERNAL	STERNUM	1.50
E INTERNAL	R RIB	1.50
F INTERNAL	L RIB	1.50

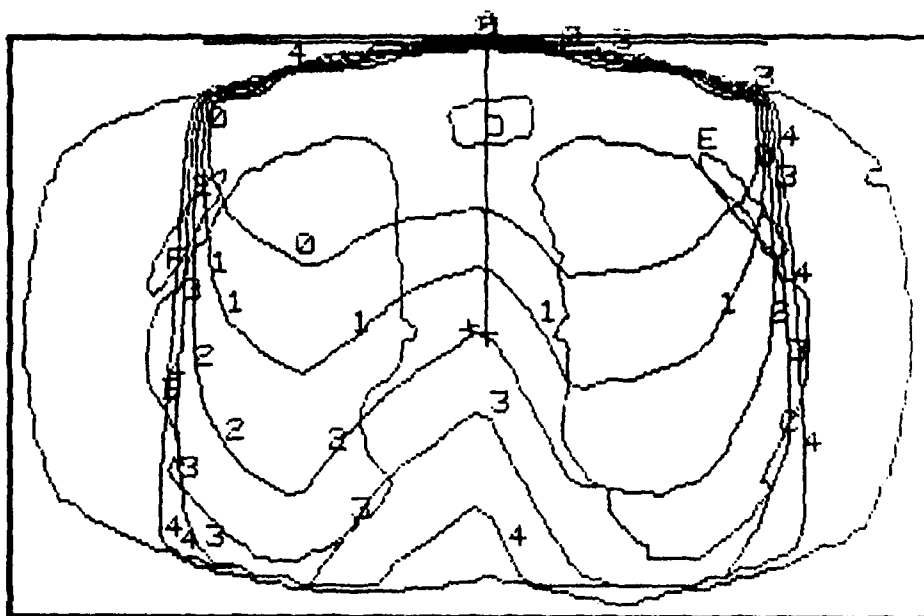


Fig. 23. Contours and Isodose Curves for CT outline of Rando Slice 14

PATIENT ID:	RT3	PHANTOM, RANDO
PLAN ID:	WORKAREA - 1	WORKAREA - 1
X-SEC:	GESL35	GE SLICE 35

DISPLAY NORMALIZATION = STANDARD
DOSE = 150.00

MAX. IN WINDOW = 267

NOTE: SSD FIELD SIZE ON SKIN
SAD/ROT FIELD SIZE AT ISOCENTER

MACHINE TYPE.....	1
BEAM TYPE.....	COBALT
SOURCE-SKIN DISTANCE (MM)	SAD
SOURCE-AXIS DISTANCE (MM)	915.00
FIELD WIDTH (MM).....	250.00
FIELD LENGTH (MM).....	250.00
OFF-AXIS DISTANCE (MM)...	.00
WEIGHT.....	150
IGNORE CONTOUR.....	NONE
WEDGE #1 ID.....	
NORMALIZATION.....	
SYMMETRY.....	
WEDGE #2 ID.....	
NORMALIZATION.....	
SYMMETRY.....	
ENTRY POINT	
X (MM).....	6.00
Y (MM).....	111.87
ISOCENTER	
X (MM).....	6.00
Y (MM).....	-1.00
ENTRY ANGLE.....	90
ROTATION ARC.....	
SWIVEL ANGLE.....	0
PORT ROTATION ANGLE.....	0
SKIN-AXIS DIST (MM, W/COR)	120.94
ISOCENTER TAR/TMR (W/CDR)	.7487
SKIN-AXIS DIST (MM, N/COR)	112.94
ISOCENTER TAR/TMR (N/COR)	.7742

Fig. 22. Treatment Plan for Actual CT Outline
of Rando Slice 14

The treatment plan is shown in Fig. 18. This illustrates the beam properties defined earlier. From the calculated dose, isodose curves were generated over the contour outline (Fig. 19).

For the purpose of modifier design, dose data are needed only at the TLD (tumor) locations ($Y=0$). The calculated distribution along this line is illustrated in Fig. 20. The dose was read from this distribution at points that coincide with TLD locations. The distribution was then normalized to the minimum dose. The resulting normalized dose distribution is compared to the actual dose profile in Fig. 21.

The shape of the distribution resembles the actual dosimetry data. The maximum deviation from measured dose (7%) is near the beam edge. The next step was to enter the contour data directly from a CT scan of the same section, and observe the change.

The surface and internal contours were outlined directly on a CT scan of the phantom slice. The same anterior beam was defined for the computer. The resulting treatment plan is shown in Fig. 22. The contours and isodose curves are available in Fig. 23. Fig 24 shows the dose distribution along the tumor plane (in this case, the negative and positive x values are reversed). This distribution was normalized to the minimum dose and is compared to the actual dosimetry in Fig 25.

As before, the shape of the dose profile is similar to the measured shape. But still some discrepancies are visible. The final distributions were obtained after many attempts to accurately define the contours and densities. It was concluded that, given accurate

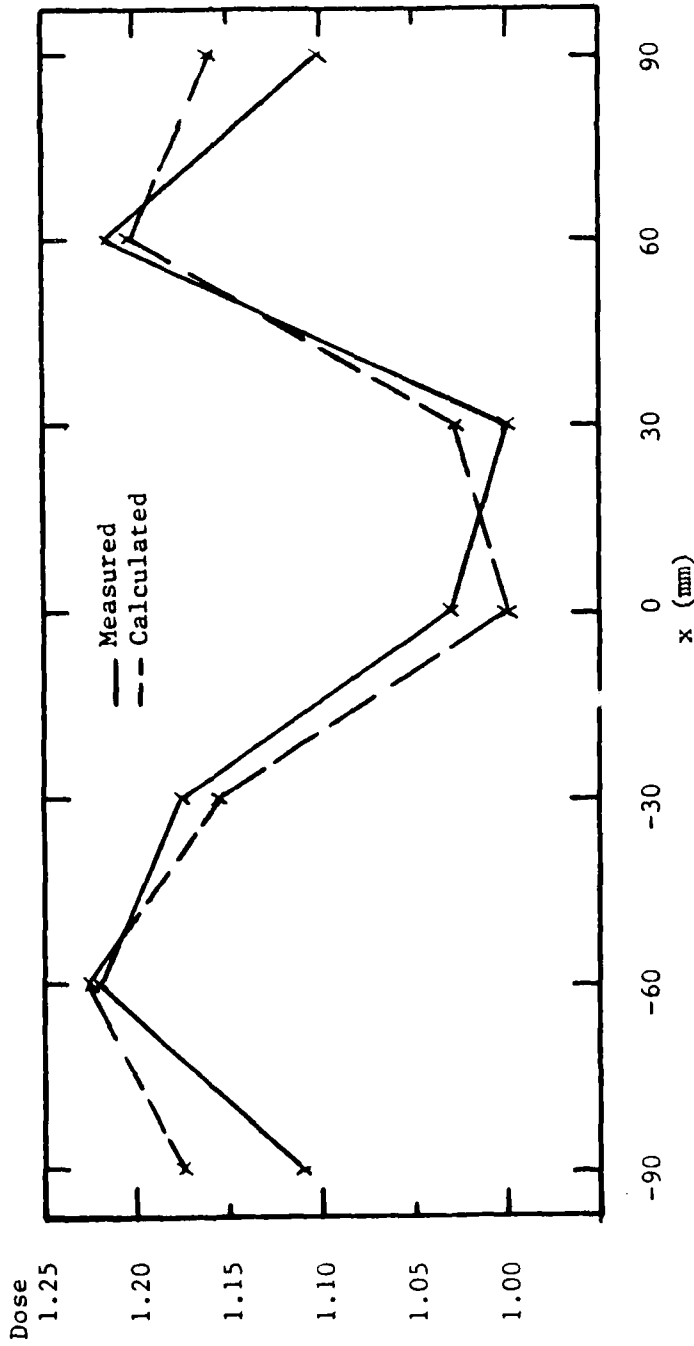


Fig.21. Comparison of Calculated and Measured Dose Distributions

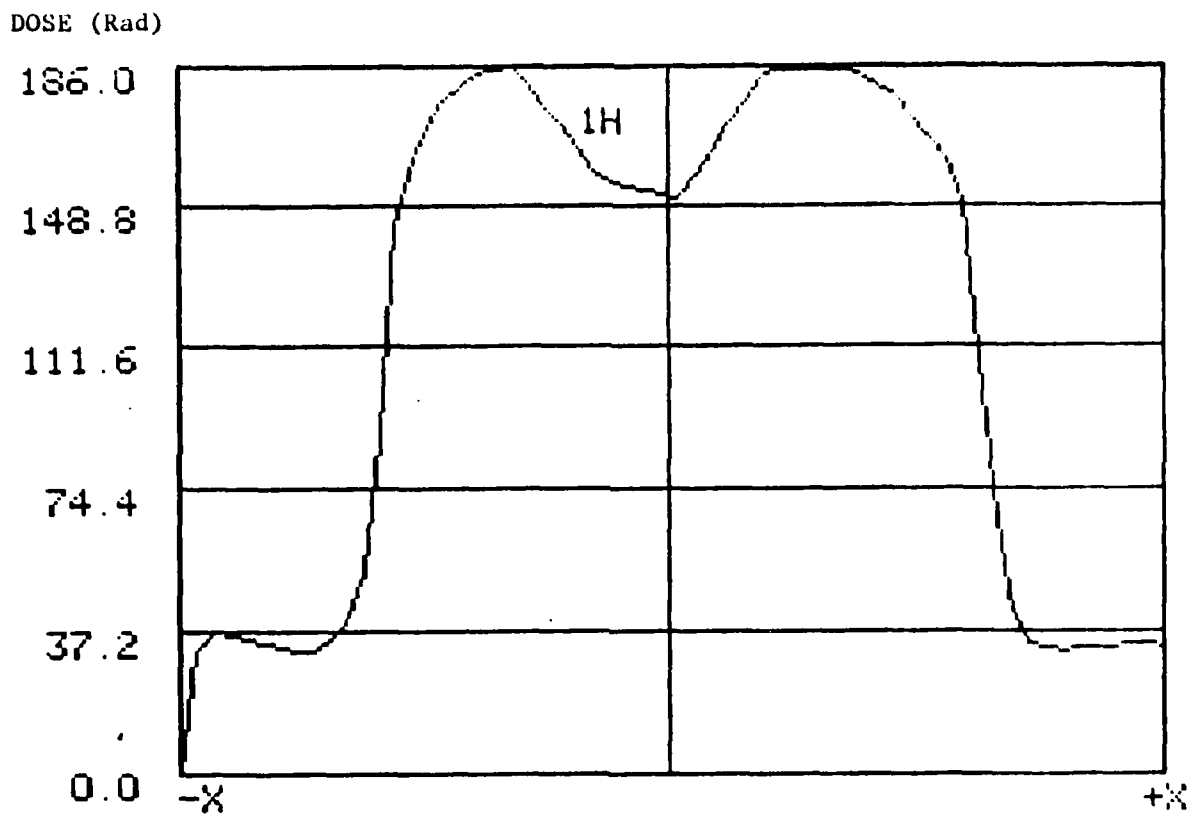


Fig. 20. Calculated Dose Distribution Along Tumor Plane

ISODOSE	0	1	2	3	4
VALUES	200	175	150	125	100

CONTOUR	DESCRIPTION	DENSITY GM/CC
A PATIENT	SURFACE	1.00
B INTERNAL	LEFT LUNG	.30
C INTERNAL	RIGHT LUNG	.30
D INTERNAL	STERNUM	1.50
E INTERNAL	LEFT RIB	1.50
F INTERNAL	RIGHT RIB	1.50

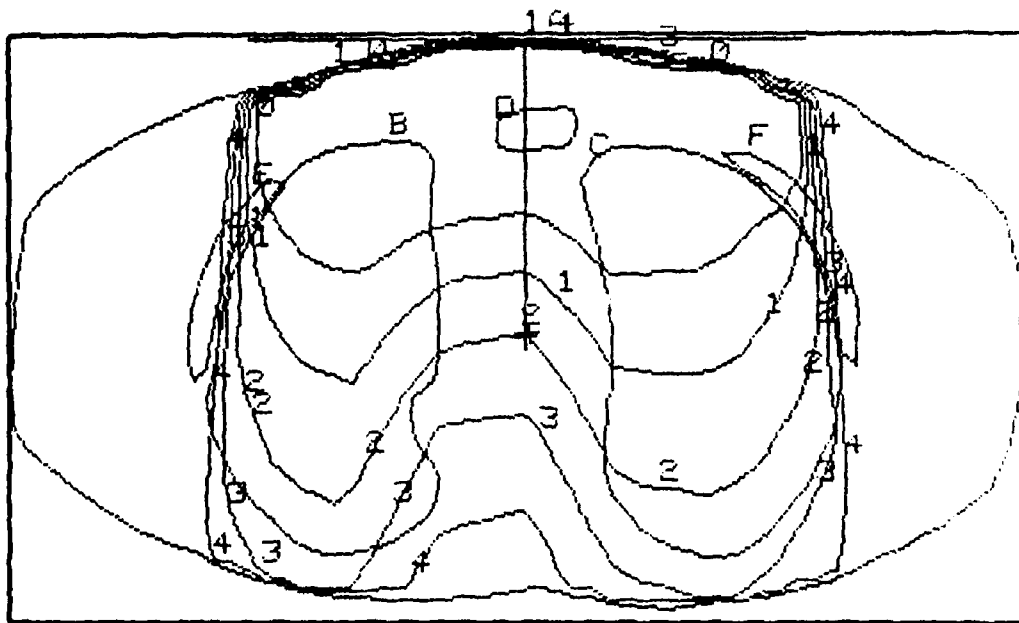


Fig. 19. Contours and Isodose Curves for x-ray print of Rando slice 14

PATIENT ID: RT2	RANDO, PHANTOM
PLAN ID: WORKAREA - 1	WORKAREA - 1
X-SEC: SL14	CONTACT XRAY PRINT

DISPLAY NORMALIZATION = STANDARD
DOSE = 150.00

MAX. IN WINDOW = 276

NOTE: SSD FIELD SIZE ON SKIN
SAD/ROT FIELD SIZE AT ISOCENTER

MACHINE TYPE.....	1 COBALT
BEAM TYPE.....	SAD
SOURCE-SKIN DISTANCE (MM)	
SOURCE-AXIS DISTANCE (MM)	915.00
FIELD WIDTH (MM).....	250.00
FIELD LENGTH (MM).....	250.00
OFF-AXIS DISTANCE (MM)...	.00
WEIGHT.....	150
IGNORE CONTOUR.....	NONE
WEDGE #1 ID.....	
NORMALIZATION.....	
SYMMETRY.....	
WEDGE #2 ID.....	
NORMALIZATION.....	
SYMMETRY.....	
ENTRY POINT	
X (MM).....	-1.00
Y (MM).....	115.00
ISOCENTER	
X (MM).....	-1.00
Y (MM).....	.00
ENTRY ANGLE.....	90
ROTATION ARC.....	
SWIVEL ANGLE.....	0
PORT ROTATION ANGLE.....	0
SKIN-AXIS DIST (MM, W/COR)	122.81
ISOCENTER TAR/TMR (W/COR)	.7432
SKIN-AXIS DIST (MM, N/COR)	115.19
ISOCENTER TAR/TMR (N/COR)	.7670

Fig. 18. Treatment Plan for Test of Computational Accuracy

distribution from an unmodified beam is not available with real patients. If the calculated dose profile is equivalent to the actual distribution, then a modifier designed from it should work as if designed from the measured dose.

Programming is available to calculate dose distribution from unmodified beams. There are two preliminary steps in the calculation: (1)- defining surface and tissue contours from CT scans or with a tracing device, and (2)- defining the unmodified treatment beam incident on the CT slice. The computer then calculates the dose from the beam throughout the slice, taking into account surface contours, defined inhomogeneities, and scatter. If the contours and tissues are defined properly, then the resulting calculation should approximate measured data. More information about the calculational procedure is available in Appendix C.

Verification by comparing to a known measured dose in a patient is not possible. But the dose is known in the Rando phantom for a specific beam (Fig. 13) and can serve as a benchmark. This was the initial test of the calculated results.

Contour information was entered into the computer for section #14 of the Rando phantom by tracing an x-ray contact print of the section with the tracing input device. This is the section for which actual dosimetry data are available in water (Fig. 12). The water dosimetry is used for comparison because, in calculating scatter, the computer assumes uniform unit density tissue (water) on both sides of the slice being exposed.

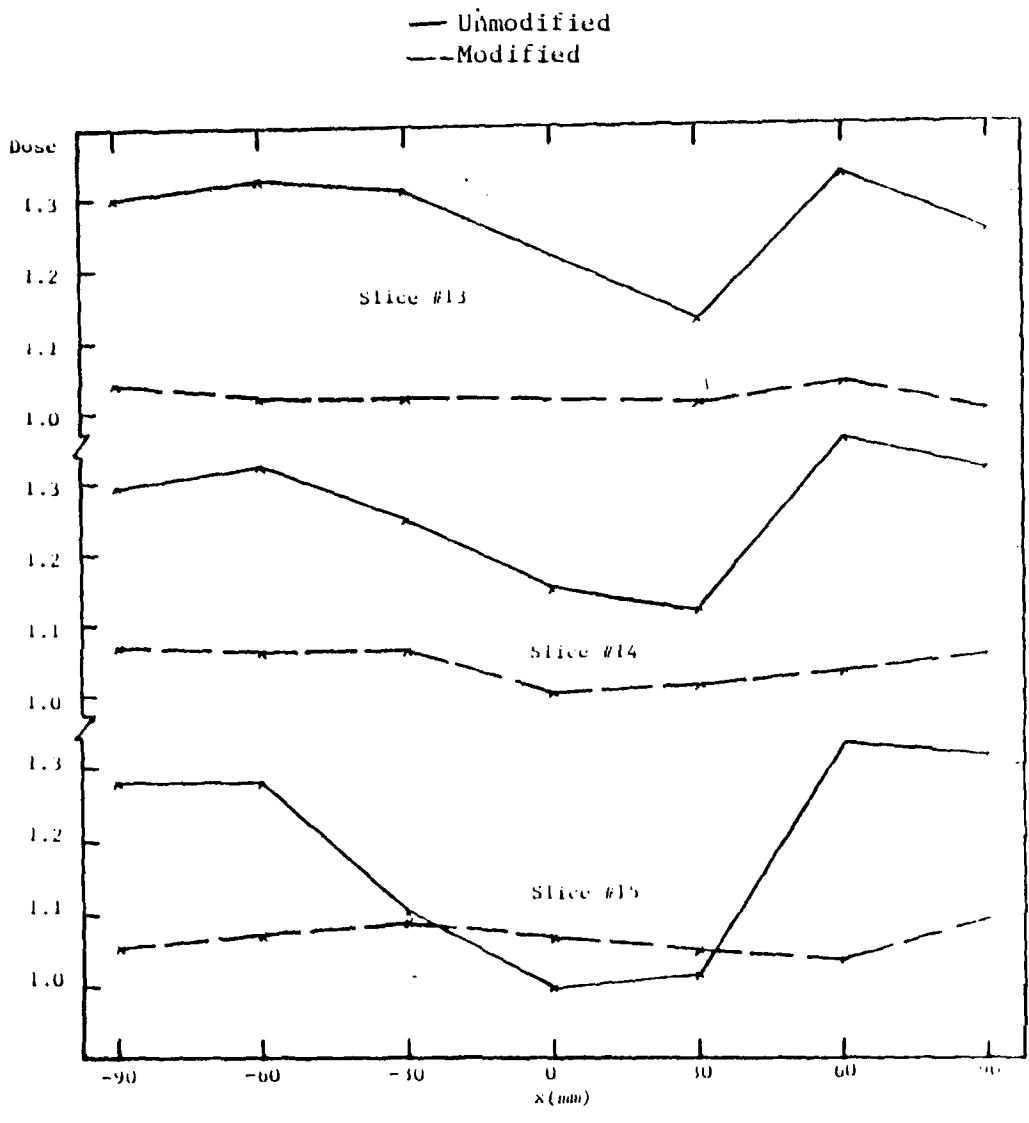


Fig. 17. Dose Distribution with and without Beam Modification

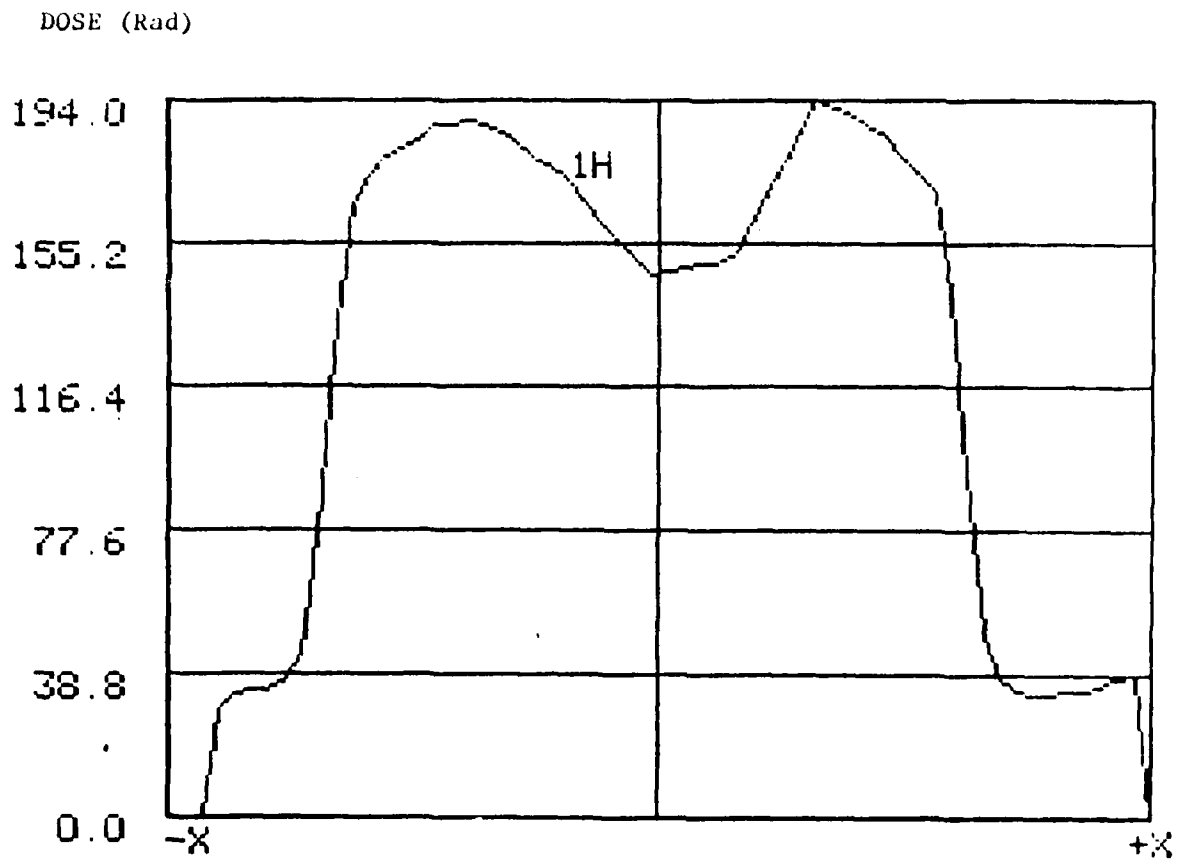


Fig. 28. Calculated Dose Distribution for Section 15

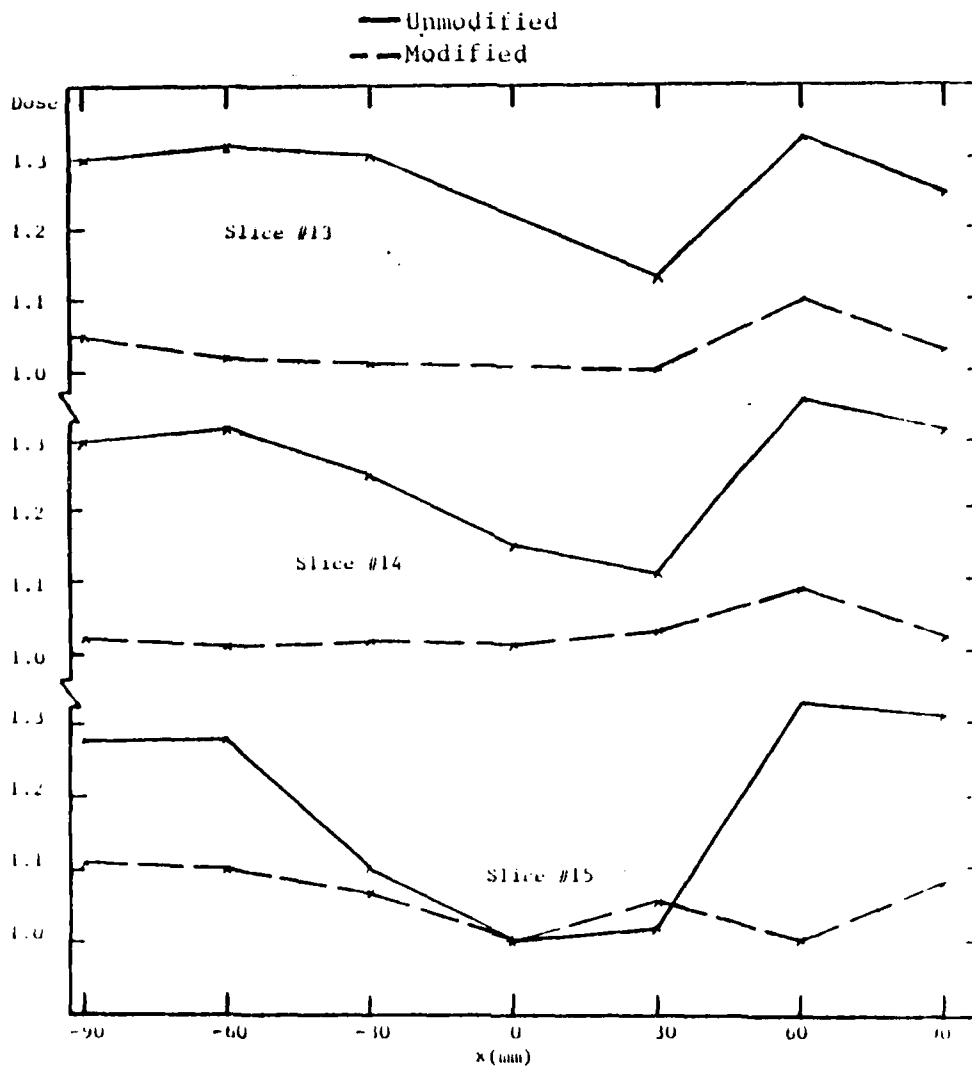


Fig. 29. Measured Dose Distribution in Three Random Sections (with and without modification)

beam. While a 10% deviation from uniformity is present on the right side, substantial 'flattening' did occur.

The deviation from uniformity results from several factors, some of which are:

1. The gaps in the present modifier
2. Possible inaccurate definition of tissue contours and densities
3. The computer calculation ignores features adjacent to the slice which may affect dose.

IV. Conclusions

By definition, the design for beam modifiers meets three of the criteria mentioned previously: use of CT scans, use of various modifier materials, and use with different beam energies. The method can also lend itself to programmed design and automated construction, although not attempted in the present research.

Application to irregular field treatment was not investigated. Since the scatter calculation in an irregular field plan is quite complicated, the introduction of a modifier in the beam could have unanticipated effects. However, if it were possible to compute detailed dose distributions from irregular fields, they could be used in the design. Since current irregular field plans don't include inhomogeneities, a modifier designed from the information in the patient could be a marked improvement.

Application to external beam treatments has been demonstrated. The design can deliver a prescribed dose distribution (within 10%). A continuous modifier material should provide further improvement. Future modification in the computer's ability to calculate dose will not make this design obsolete. On the contrary, any additional accuracy in the unmodified dose distribution (used as a starting point) will only enhance the ability of the design to deliver the prescribed dose in the patient.

V. Reccomendations

There are several tasks that should be accomplished before the design can be verified as meeting all six criteria.

The first test, discussed in Appendix B, should be the application to a 'tumor volume' as opposed to a 'tumor plane'. This would further illustrate the success of the design in meeting the first and most important criteria: delivering the prescribed dose.

Another extension would be to use a continuous modifier material. The use of a continuous modifier would automatically remove the gaps in the present construct. It would also allow a more precise design to be used. Also, if the material could be formed from a styrofoam mold, automated construction could be added.

A third improvement would be to increase the accuracy of the calculated dose distribution. The most obvious way to improve the result is to use more accurate densities and contours in the program. Any improvements here would have immediate results on the improved ability of the modifier to deliver the prescribed dose. This is because the design would be based on more realistic information about what is happening inside the patient.

Three-dimensional treatment planning would be the best amendment to the method. Currently, the modifier is designed for each CT slice independently. Treatment planning that includes adjacent slices would provide the most accurate basis for the design of the modifier.

If 3-D planning were available, actual dose profiles would be used for irregular fields. This would enable the design to use the

same method developed in this research (without any complicated iterations for scatter). Also, the dose information from external beam plans would be more reliable, by considering adjacent features that affect the dose profile.

The impact of greater accuracy would also be noticed clinically. According to Stewart, "...small errors in correctly computing and delivering dose can have catastrophic results in terms of failure to control the patient's disease." and since "...about one-third of cancer deaths result directly from failure to control local-regional sites of involvement."(1:315), there is room for improvement.

Appendix A: Effect of Contour on Beam Uniformity

A test was performed to determine the singular effect of surface contour on the dose profile in the patient. This was accomplished by defining two 'patients' on the computer.

The first patient has a rectangular external contour, and is of homogeneous, unit density (water). The surface exposed to the beam is the ideal flat, orthogonal plane approximated by a simple tissue compensator.

The second patient was an actual outline of a Rando phantom CT scan. All internal tissue was assigned unit density. This means the only difference between the two 'patients' is the shape of the surface exposed to the beam.

The dose to each slice was from the same incident beam. The resulting isodose curves are shown with the contours in Figs. 30 & 31. The dose distribution along the horizontal axis (tumor plane) of each patient is available in Figs. 32 & 33.

The beam is obviously flatter for the Rando phantom slice. If uniform dose is the goal, then a patient shaped as a flat surface orthogonal to the beam is not necessarily ideal. Indeed, if the lateral tissue 'deficits' were compensated for, the beam would lose uniformity and approach that of Figs. 30 & 32. Intuitively, this can be explained by recalling that the diverging beam can be imagined having a convex-downward shape (points of equal intensity are bowed downward toward the patient). This shape is best 'flattened' by an equivalent convex upward surface (similar to that of the body).

ISODOSE VALUES	0	1	2	3	4	5	6
	90	80	70	60	50	40	30

CONTOUR	DESCRIPTION	DENSITY
A PATIENT	SURFACE	GM/CC
		1.00

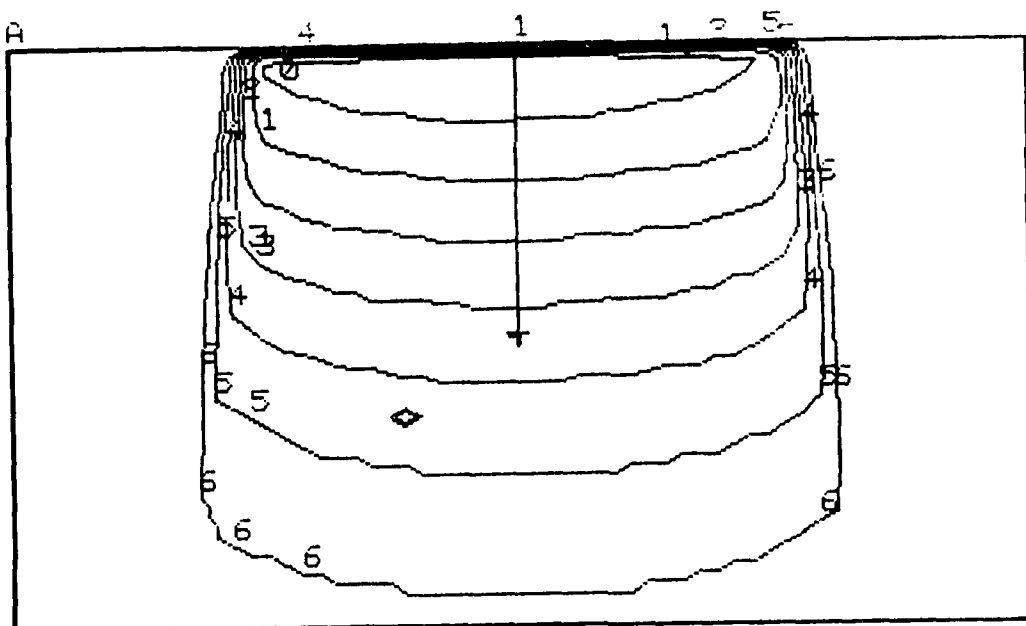


Fig. 30. Contour and Isodose Curves for a Flat Homogeneous Patient

ISODOSE	0	1	2	3	4	5	6
VALUES	90	80	70	60	50	40	30

CONTOUR	DESCRIPTION	DENSITY GM/CC
A PATIENT	SURFACE	1.00
B INTERNAL	LEFT LUNG	1.00
C INTERNAL	RIGHT LUNG	1.00
D INTERNAL	STERNUM	1.00
E INTERNAL	LEFT RIB	1.00
F INTERNAL	RIGHT RIB	1.00

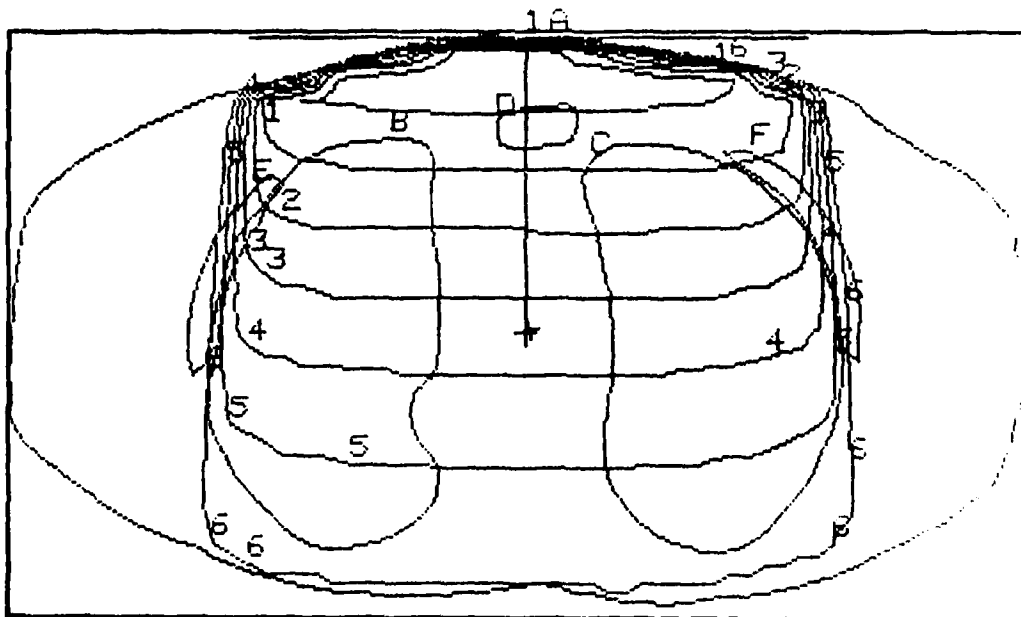


Fig. 31. Contours and Isodose Curves for a Homogeneous Patient with Actual Rando Phantom Surface

DOSE (Rad)

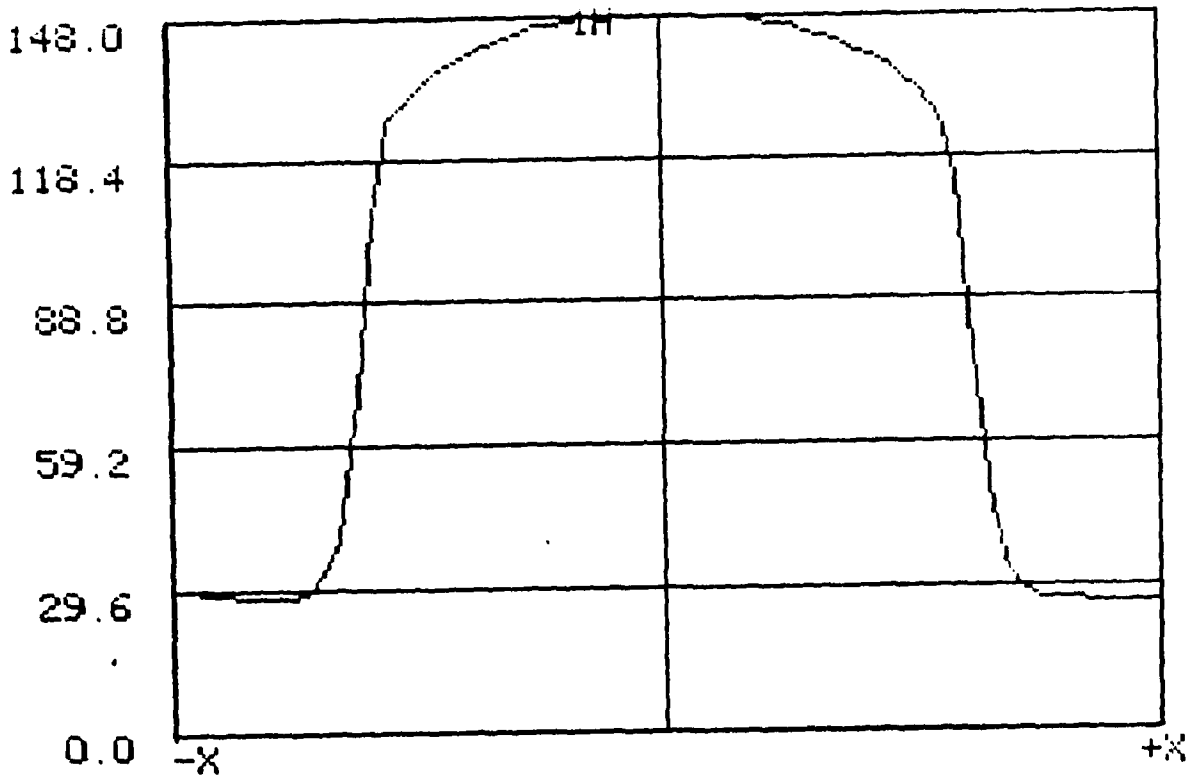


Fig. 32. Calculated Dose Distribution at Midplane for a 'flat' patient

DOSE (Rad)

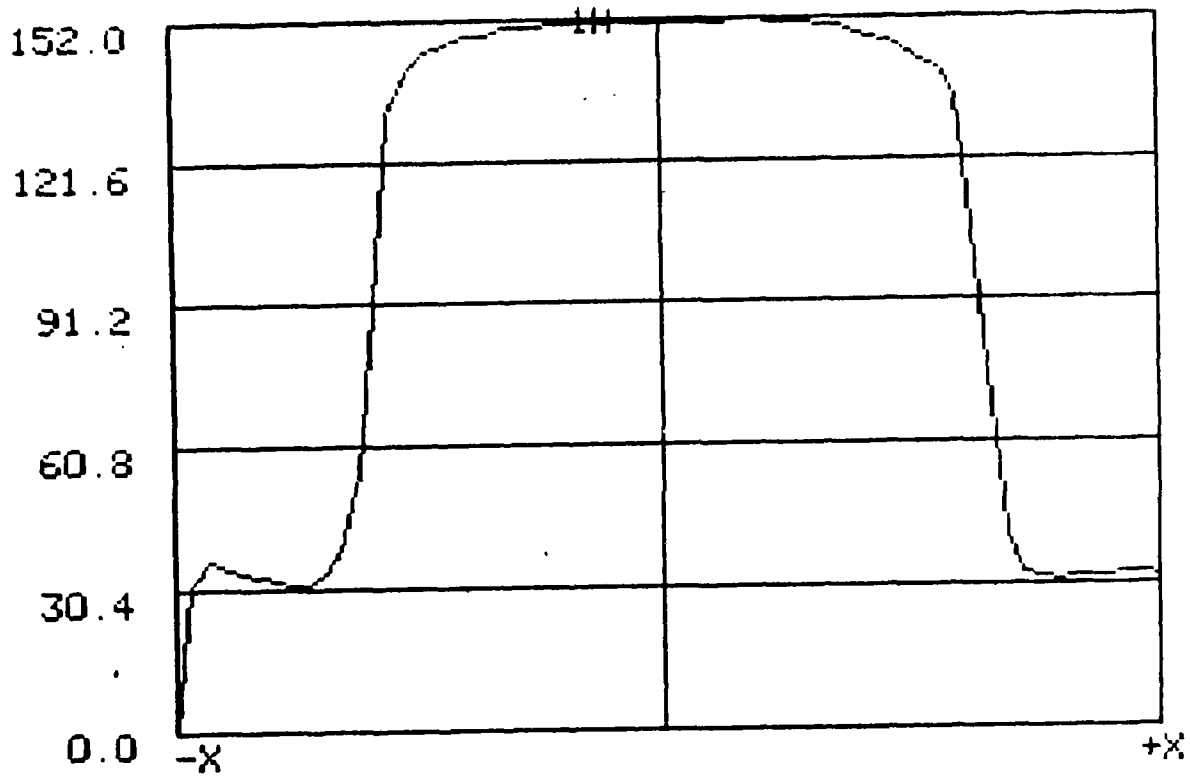


Fig. 33. Calculated Dose Distribution At Midplane for a Homogeneous Rando Phantom Section

The conclusion to be drawn is that attempts to deliver a uniform dose to the patient should consider the inherent effect of the body on beam profile. Automatically compensating for tissue deficits, without considering beam properties in the patient, can actually make matters worse.

Therefore, beam modifiers should be designed from dose information within the patient. Such a design will inherently deliver dose profiles with surface contours already considered.

Appendix B: Application to Non-planar Tumors

In demonstrating the modifier design, the prescribed dose distribution was a uniform dose at a 'tumor plane'. While this is sometimes done clinically, it is not generally the case. More often, a tumor volume or curved surface in the patient is targeted for the dose.

The design for the modifier can be extended to these general cases. This appendix discusses the extension of the method to a curved surface target. The same technique could be applied to a tumor volume by recalling that a volume is defined by its surfaces. Each beam could be shaped by the modifier to fit that beam's prescribed distribution at the volume's surface.

A typical contour is shown in Fig. 34. Instead of the usual uniform dose at a plane, a uniform dose (eg. 50 rad) is required along a 'stepped' surface.

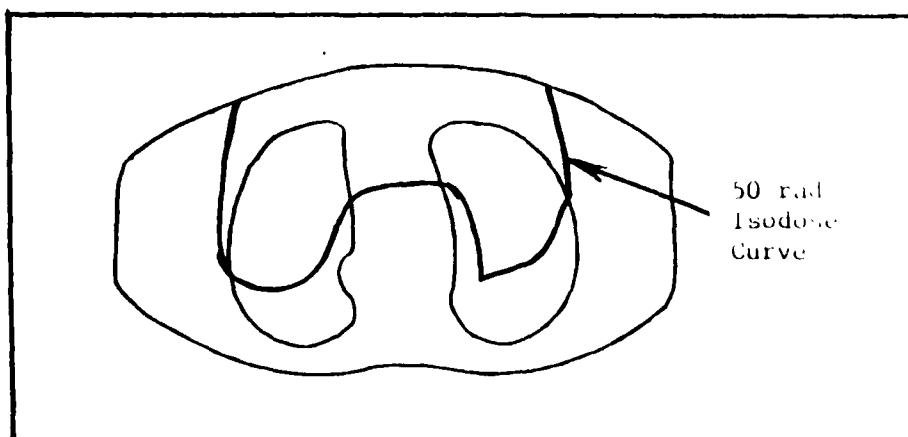


Fig. 34. Prescribed Dose Distribution

As before, the unmodified isodose curves are available from the computer. The unmodified, 50 rad isodose curve is shown in Fig. 35.

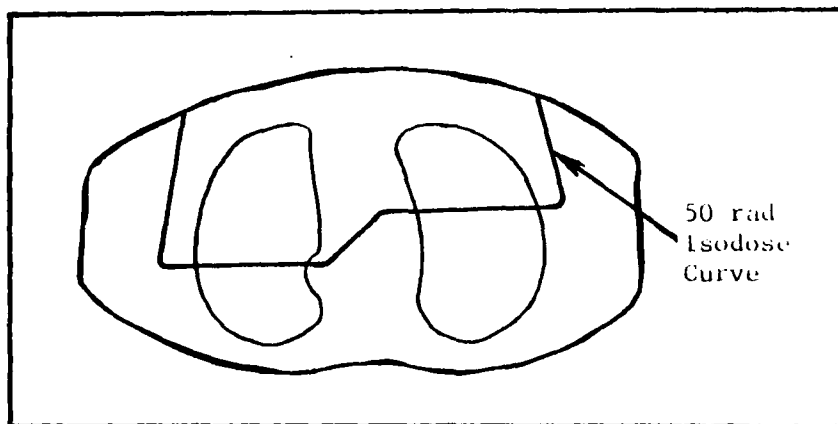


Fig. 35. Unmodified Dose Distribution

The procedure for designing the modifier begins by identifying representative points at the tumor surface for calculation (Fig. 36). The desired normalized dose at each point is 1.0.

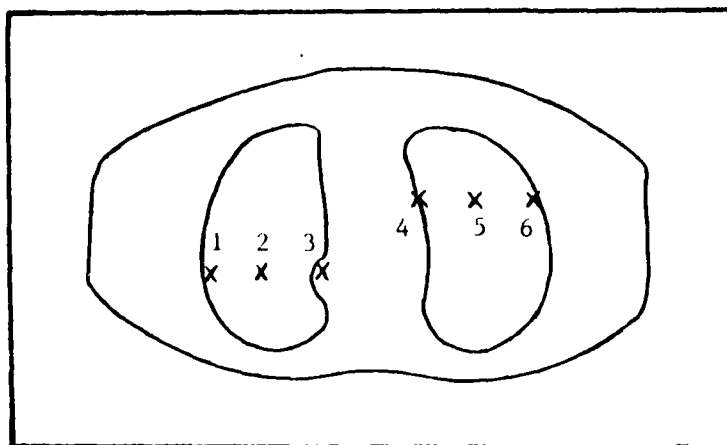


Fig. 36. Representative Tumor Points

ISODOSE	0	1	2	3
VALUES	200	175	150	125

CONTOUR	DESCRIPTION	DENSITY GM/CC
A PATIENT	SURFACE	.98
B INTERNAL	RIGHT LUNG	.32
C INTERNAL	LEFT LUNG	.32
D INTERNAL	RIGHT RIB	1.10
E INTERNAL	LEFT RIB	1.10
F INTERNAL	STERNUM	1.10

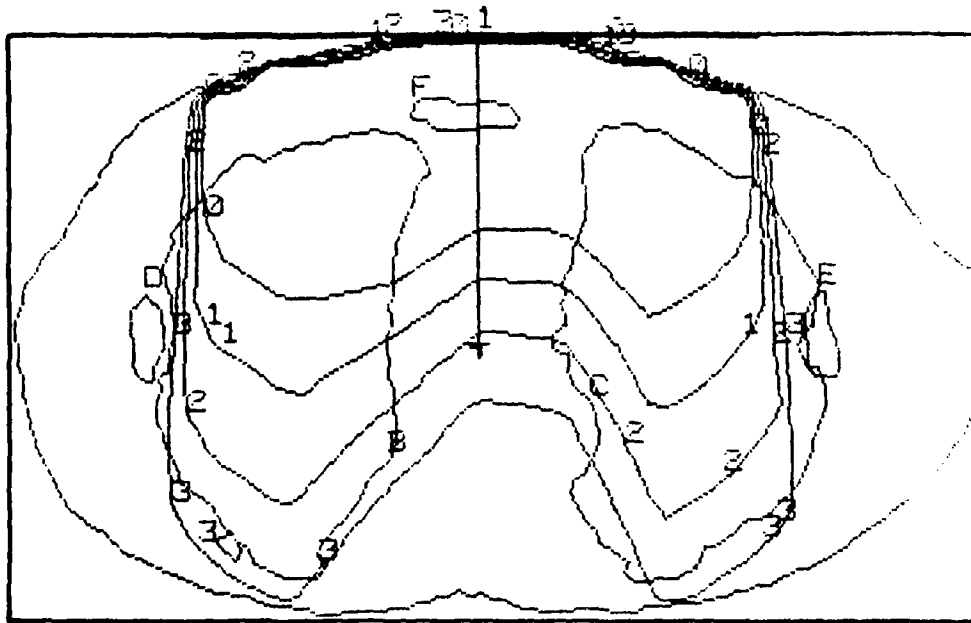


Fig. 42. Contours and Isodose Curves for Section 15

DOSE	0	1	2	3
VALUES	200	175	150	125

CONTOUR	DESCRIPTION	DENSITY GM/CC
A PATIENT	SURFACE	98
B INTERNAL	RIGHT LUNG	32
C INTERNAL	LEFT LUNG	32
D INTERNAL	RIGHT RIB	1.10
E INTERNAL	LEFT RIB	1.10
F INTERNAL	1.1	1.10

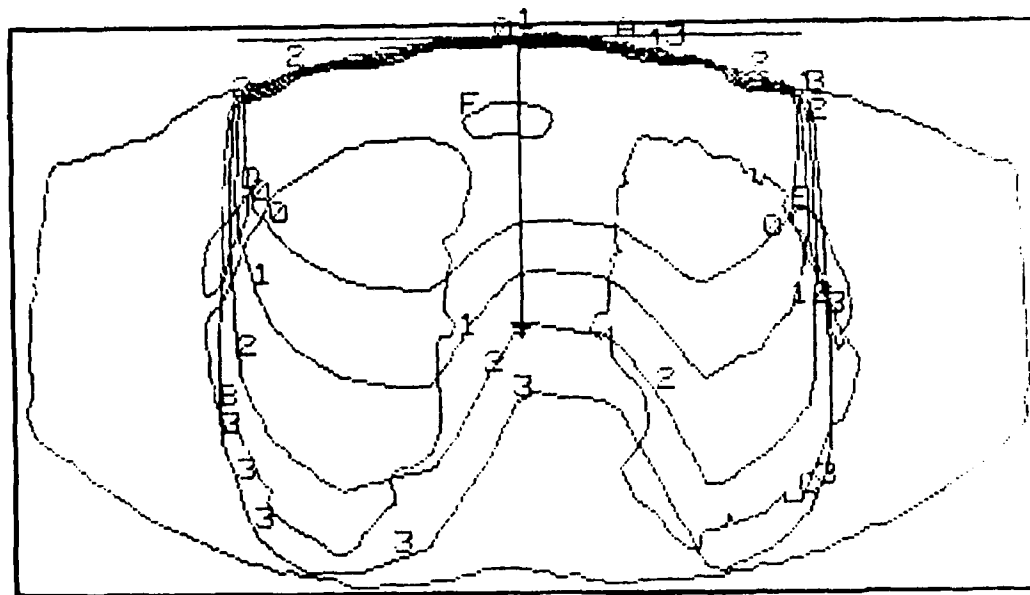


Fig. 41. Contours and Isodose Curves for Section 14

ISODOSE	0	1	2	3
VALUES	200	175	150	125

CONTOUR	DESCRIPTION	DENSITY GM/CC
A PATIENT	SURFACE	0.98
B INTERNAL	RIGHT LUNG	0.37
C INTERNAL	LEFT LUNG	0.37
D INTERNAL	RIGHT RIB	1.20
E INTERNAL	LEFT RIB	1.20
F INTERNAL	STERNUM	1.30
G INTERNAL	TRACHEA	0.00
H INTERNAL	SCAPULA	1.20
I INTERNAL	SCAPULA	1.20

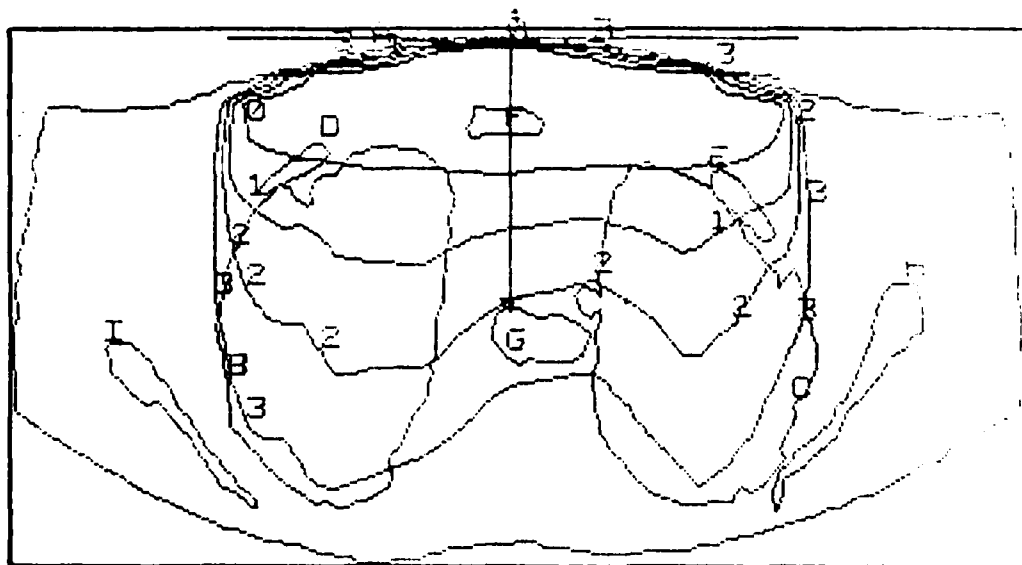


Fig. 40. Contours and Isodose Curves for Section 13

PHANTOM, RANDO WINDOW: 207 X 400
 WORKAREA - 1 X, Y: 3 , 1
 RANDO SLICE 13 (GE SL4) MATRIX: 60 X 60

DISPLAY NORMALIZATION = STANDARD
 DOSE = 150.00

MAX. IN WINDOW = 248

NOTE: SSD FIELD SIZE ON SKIN
 SAD/ROT FIELD SIZE AT ISOCENTER

MACHINE TYPE.....	1 COBALT
BEAM TYPE.....	SAD
SOURCE-SKIN DISTANCE (MM)	
SOURCE-AXIS DISTANCE (MM)	915.00
FIELD WIDTH (MM).....	250.00
FIELD LENGTH (MM).....	70.00
OFF-AXIS DISTANCE (MM)...	25.00
WEIGHT.....	150
IGNORE CONTOUR.....	NONE
WEDGE #1 ID.....	
NORMALIZATION.....	
SYMMETRY.....	
WEDGE #2 ID.....	
NORMALIZATION.....	
SYMMETRY.....	
ENTRY POINT	
X (MM).....	5.25
Y (MM).....	101.25
ISOCENTER	
X (MM).....	.00
Y (MM).....	.00
ENTRY ANGLE.....	87
ROTATION ARC.....	
SWIVEL ANGLE.....	0
PORT ROTATION ANGLE.....	0
SKIN-AXIS DIST (MM, W/COR)	93.25
ISOCENTER TAR/TMR (W/COR)	.7438
SKIN-AXIS DIST (MM, N/COR)	101.62
ISOCENTER TAR/TMR (N/COR)	.7119

Fig. 39. Sample Treatment Plan for Computational Validation of Design

Appendix E: Additional Dose Profiles Used In
Calculational Validation

The figures in this appendix provide more detailed information about the computer results used as a basis for the modifier design. Fig. 39 is a sample treatment plan used to generate the calculational results. Figs. 40-42 show the contours and isodose lines for the three slices under consideration. Figs. 43-45 show an isometric plot of the dose profile for each CT slice.

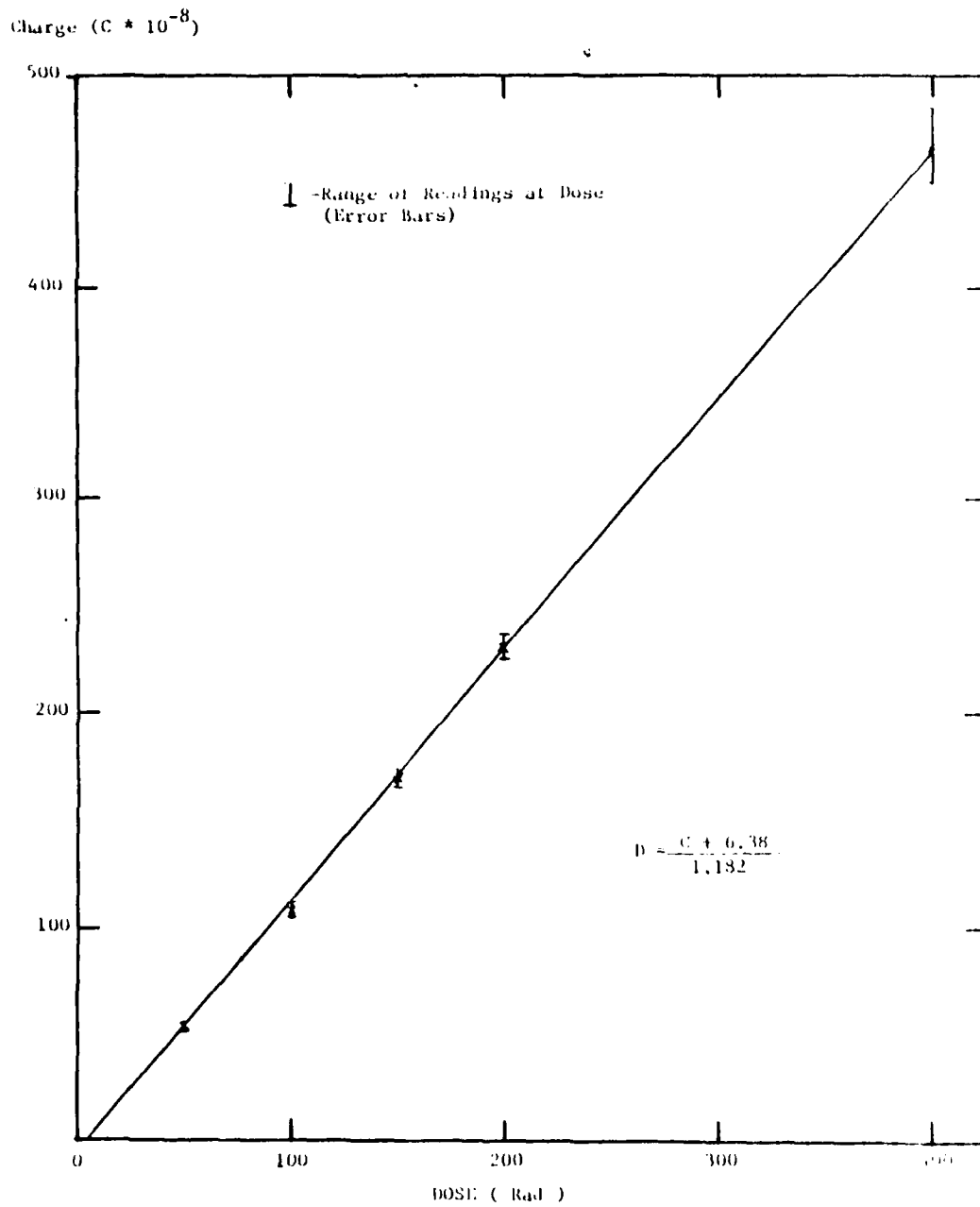


Fig. 38. TLD Calibration Curve

The pairs were then calibrated to various known doses. This allows the relationship between the reading and the actual dose to be determined. The calibration curve relating charge to dose is shown in Fig. 38. Accuracy could only be determined empirically, so no theoretical confidence level is available. However, all exposures to a known dose were always within 3% of the value predicted by the calibration curve.

For the purposes of this research, accuracy of dose was not as critical as precision, since absolute dose was rarely needed. The concern was primarily with the relative (normalized) dose from each exposure.

The dosimeters used in this research were TLD-100 rods (manufactured by the Harshaw Chemical Co.). They were placed in gelatin capsules for exposure in the Rando phantom. The light emitted from the heated TLD's was converted to a current and recorded by a Harshaw 2000D Automated TL Analyzer System. The dosimeters were annealed at 400°C for one hour after each use to remove any residual radiation effects.

Statistics

To improve the precision of the measurements, the TLD's were paired. The average reading (dose) from a pair was used. The pairs were selected after many individual exposures to a known dose. For instance, a TLD that read consistently high by 3% was paired with one that consistently read 3% low. The precision of this method was calculated by exposing the pairs and recording the results.

The following table shows the results from an exposure to a known dose (100 rad). A batch refers to 15 pairs of TLD's. The integrated charge (related to dose later) recorded by the Harshaw system is the reading

<u>Batch</u>	<u>Mean Reading</u> <u>C * 10**⁻⁸</u>	<u>Standard</u> <u>Deviation (%)</u>	<u>99% Confidence</u> <u>(3 * S.D.)</u>
A	125.0	0.98 (0.78)	2.35 %
B	123.1	0.89 (0.72)	2.17
C	124.0	1.01 (0.81)	2.44
D	123.9	1.15 (0.93)	2.78
E	122.2	1.54 (1.26)	3.18

Appendix D: TLD Theory and Statistics

All dose measurements in this research were made with TLD's (Thermoluminescent Dosimeters). TLD's are substances that, when exposed to ionizing radiation, store energy. That stored energy is released as light upon subsequent heating. The amount of light released (fluorescence) can be related to the amount of radiation absorbed.

Theory

Electrons in a TLD are confined to certain energy states (conduction band and valence band). Impurities in the crystal create electron states in the band gap. When irradiated, some of these locations trap electrons. Adding heat allows the electrons to escape and fall into the valence band, producing a thermoluminescent photon. This light can be measured with a photomultiplier tube and an ammeter.

Lithium Fluoride (LiF) crystals are often used as TLD's. LiF has several desirable characteristics for dosimetry. Some of these are listed below.

- Convenient, small form
- Wide range of sensitivity (1mR to 10^5 Rad)
- Almost tissue-equivalent
- Minimal dependence on dose rate
- Reusability
- Long-term information retention

Application to Modifier Design

Each type of treatment plan has advantages and drawbacks. Presently, the I.F. technique cannot be used for designing modifiers. Recall that the starting point for the design is a calculated dose distribution from the unmodified treatment beam. Such detailed information is not available from the I.F. calculations. Also, compensation for density differences would not be possible, since the I.F. calculation doesn't include them. However, an approximate modifier designed from an equivalent rectangular beam might be used for I.F. treatments. As mentioned in the recommendations, this should be investigated.

Since a dose distribution is available, and surface contours and density differences are included, the results from the EB calculation should be used in the design. This, however, is not ideal, since the modifier must be designed independently for each CT slice in the beam's field. Until 3-D treatment planning is available, this must suffice.

Eventually, a calculation is needed that combines the best features of both techniques: (1)-Patient data from CT as in the EB method, and (2)-Beam data and scatter calculations that include adjacent tissue as in the I.F. method.

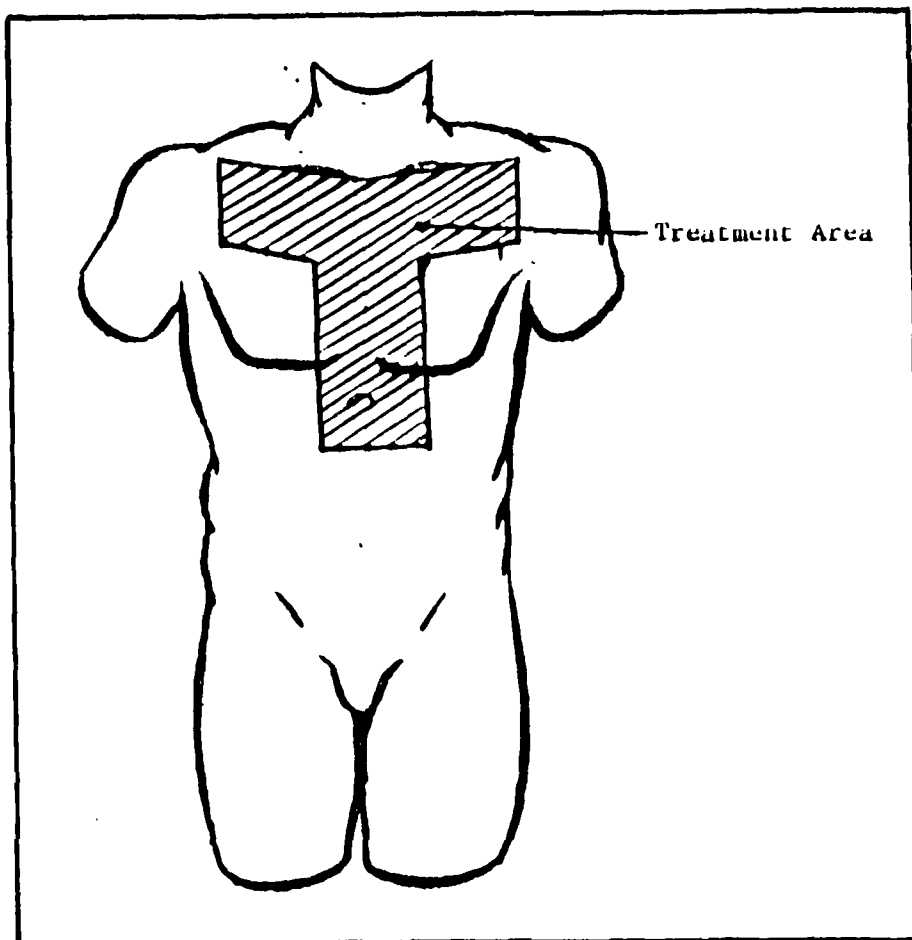


Fig. 37. Typical Irregular Field Treatment Area

The radiotherapist selects several points of interest within the field for dose calculation. The computer then calculates the primary and scatter dose at various depths beneath each point. Although the program assumes a unit density throughout the field, it does account for a curved exterior surface.

Several beams are then defined to deliver the specified dose distribution (The fewer beams, the better). These beams are manipulated until the calculated dose at the target volume is acceptable. Several parameters may be changed to achieve the desired result. They

are... 1. Number of beams
2. Beam sizes
3. Beam directions
4. Beam weights (relative dose from each beam)
5. Beam modifiers (blocks, wedges, & eventually this design).

When the dose distribution is acceptable the patient data and beam data are recorded as the treatment plan.

The program calculates the dose in the slice by assuming water on both sides of the slice. This is because the beam data for scatter were previously characterized by measuring dose in water for various rectangular fields. Adjustments for inhomogeneity are made using the Cunningham model (13).

Irregular Field Planning

I.F. treatments are usually prescribed when a rectangular beam is not acceptable or when critical organs (lungs, spinal cord) must be shielded from the primary beam. The treatment area is defined in a coronal (x-z) or sagittal (y-z) plane from an x-ray film. The treatment often uses two parallel opposed beams.

A typical treatment area is shown in Fig. 37. The treatment area is entered by using a tracing device over the x-ray film. The irregular shape of the area complicates the dose calculations. Since scatter information is available from physical dose measurements in water exposed only to rectangular beams, an approximation must be made. The most prevalent method of calculating dose in I.F. is Clarkson's method (2:Ch 10).

Appendix C: Outline of Irregular Field and External Beam Treatment Techniques

At the WPAFB Medical Center, two methods for planning radiation therapy are used: External Beams (EB) and Irregular Fields (IF). Discussion of these methods beyond the outline given here is available in Ref. 12.

External Beam Planning

The EB calculation is performed for a single CT scan. The radiotherapist indicates which CT slice is to be used for the calculation. He also outlines the tumor volume target and prescribes the dose distribution. Usually, the slice with the best tumor definition is selected. Since the patient is exposed to CT for diagnosis, the data for treatment planning is readily available.

A description of CT is given by Stewart (1:314).

Computed Tomography (CT) is the reconstruction by computer of a tomographic plane or slice of an object. A CT scanner functions by performing multiple measurements of the attenuation of x-rays in body tissues by moving an x-ray source and a detector about the patient as an integral unit. These multiple determinations of x-ray attenuation are then subjected to computer processing in order to reconstruct a cross-sectional view of the scanned object in the form of a density matrix, where each element is assigned a specific attenuation value. Display routines produce an image in which the attenuation values are represented by various shades of gray.

The CT image is entered into the treatment planning computer. The program then allows contours of important features (tumor, lung, spinal cord, etc.) to be outlined directly on the video display screen. The physical density of each feature is recorded.

The dose from an unmodified beam at each point is available from the computer calculation. For demonstration, points 1-6 are assumed to have the following typical doses.

<u>POINT</u>	<u>DOSE(rad)</u>	<u>N-NORMALIZED DOSE</u>
1	50	1.0
2	75	1.5
3	50	1.0
4	100	2.0
5	150	3.0
6	100	2.0

The amount of modifier required above each point to deliver the prescribed dose is calculated from equation (2). The horizontal dimensions of the modifier are again determined from the beam divergence.

PATIENT ID:
X-SEC.ID:

RT5
SL13

ANGLE: 210
VIEW ANGLE: 50

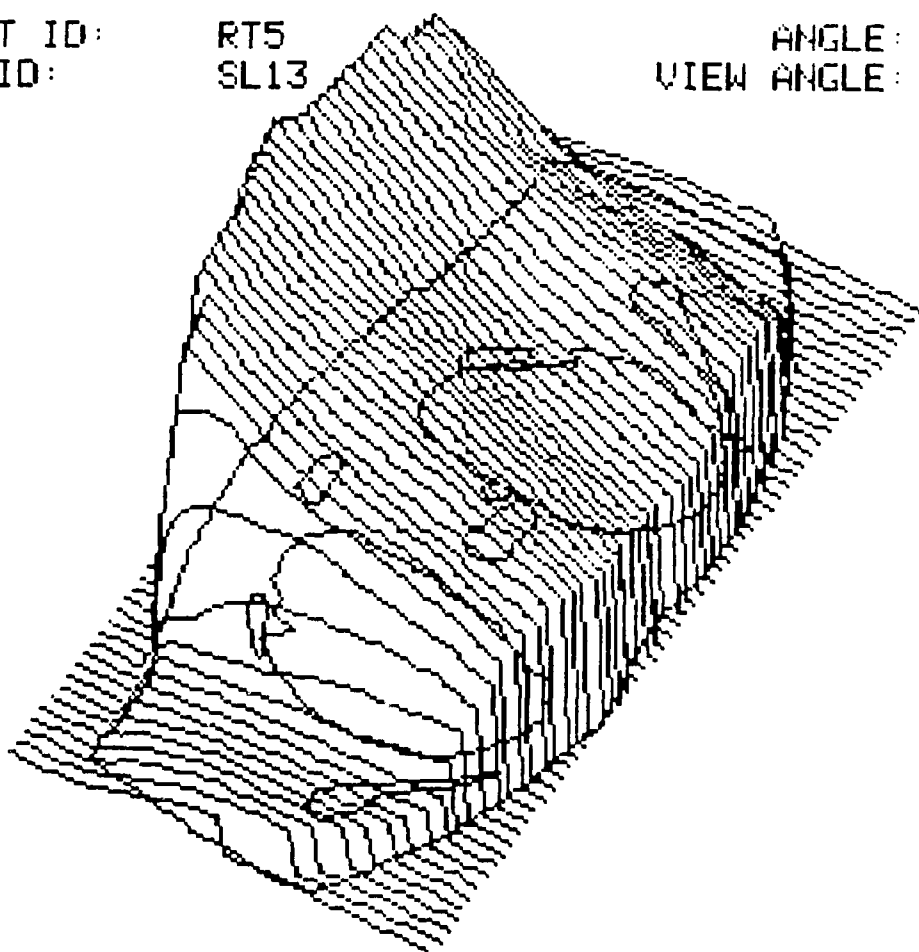


Fig. 43. Isometric Dose Profile for Section 13

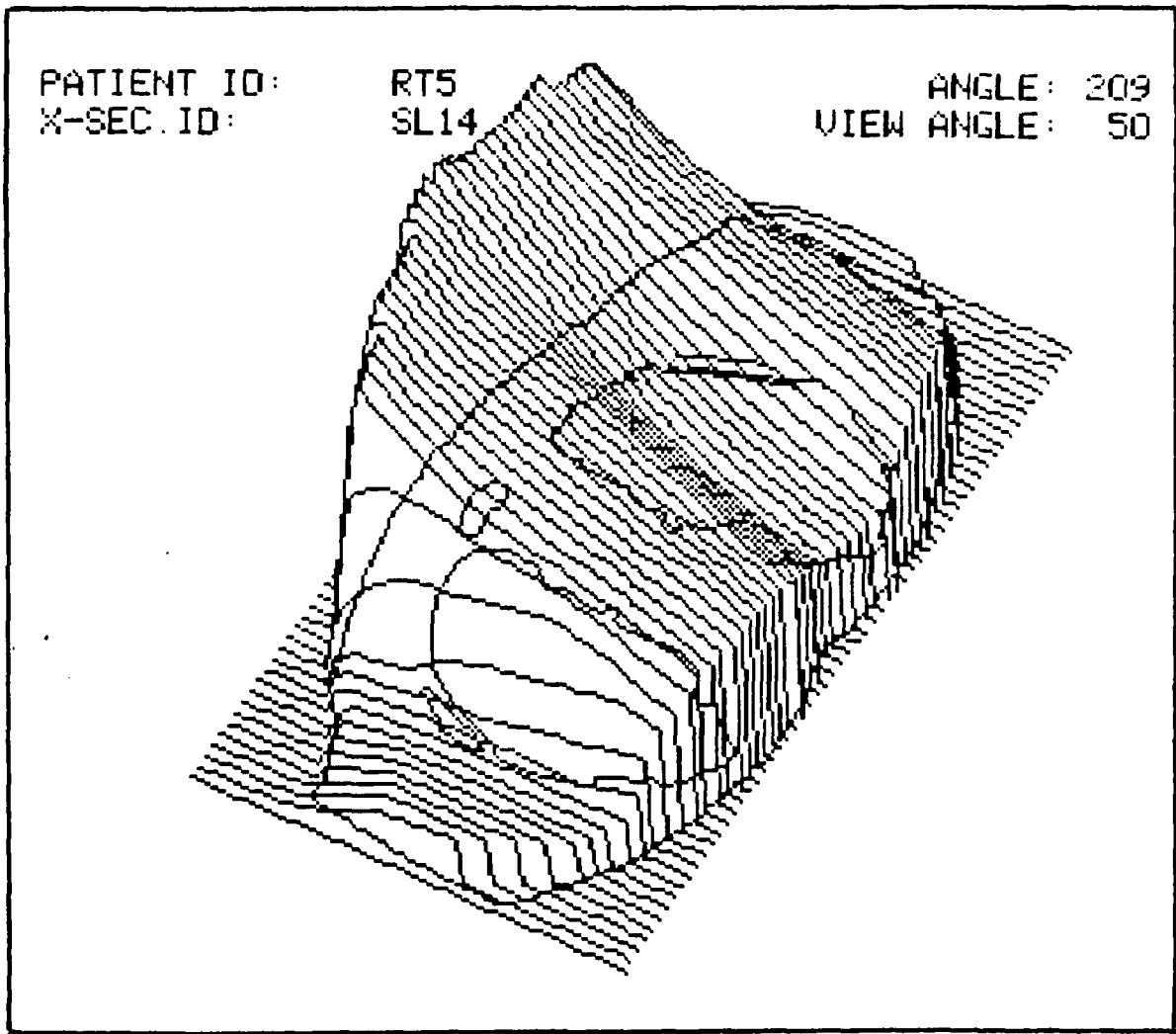


Fig. 44. Isometric Dose Profile for Section 14

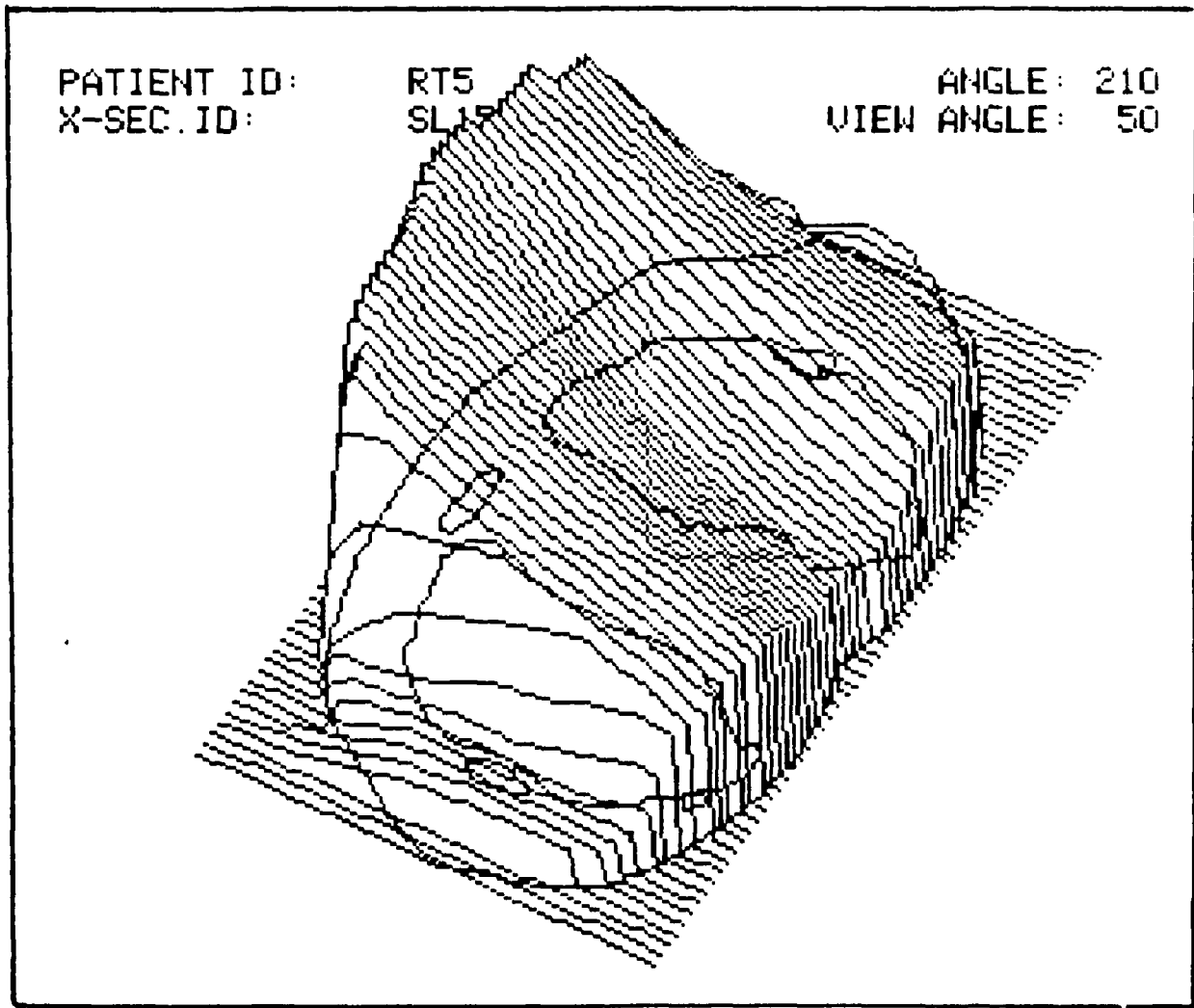


Fig. 45. Isometric Dose Profile for Section 15

Bibliography

1. Stewart, J. Robert, et al. "Computed Tomography in Radiation Therapy," Int. J. Radiation Oncology Biol. Phys., 4: 313-324, (Mar-Apr 1978).
2. Khan, Faiz M. The Physics of Radiation Therapy. Baltimore:Williams & Wilkens, (1984).
3. Leung, P.M.K. The Physical Basis of Radiotherapy. Ontario: The Ontario Cancer Institute, (1972).
4. Ellis F., et al. "A Compensator for Variations in Tissue Thickness for High Energy Beams," Br. J. Radiology 32:421-422, (Jun 1959).
5. Fletcher, Gilbert H. Textbook of Radiotherapy. Philadelphia: Lea & Febiger, (1980).
6. Boge, Jerome R., et al. "Tissue Compensators for Megavoltage Radiotherapy Fabricated from Hollowed Styrofoam Filled with Wax," Radiology, 111: 193-198, (Apr 1974).
7. Renner, W.D. "The Use of Photogrammetry in Tissue Compensator Design," Radiology, 125: 505-510, (Nov 1977).
8. Higgins, Lt. Richard. Computer Designed Compensation Filters For Use in Radiation Therapy. MS thesis, School of Engineering, Air Force Institute of Technology (AU), Wright-Patterson AFB, OH (Dec. 1982).
9. Renner, W.D., et al. "A note on designing tissue compensators for parallel opposed fields," Medical Physics, 10: 483-486, (Jul-Aug 1983).
10. Ellis, Frank and Lescrenier, Charles. "Combined Compensation for Contours and Heterogeneity," Radiology, 106: 191-194, (Jan 1973).
11. Dixon, Robert L., et al. "Compensating Filter Design Using Megavoltage Radiography," Int. J. Rad. Onc. Biol. Phys., 5:281-287 (Feb 1979).
12. RTP Release 2 Operating Manual, Part # 9861000, Computerized Medical Systems, Inc., St. Louis MO. (1982).
13. Cunningham, J.R. "Scatter-Air Ratios," Phys. Med. Biol., 17:42-51. (1972).
14. Clarkson, J.R. "A Note on Depth Doses in Fields of Irregular Shape," Br. J. Radiology, 14: 265, (1941).

VITA

Justin Keller was born in 1961 in Newport, Tennessee. He graduated from Cosby High School in June 1979. He attended the University of Tennessee in Knoxville and graduated in August 1983 with a Bachelor of Science degree in Nuclear Engineering. Upon graduation, he was commissioned in the USAF through the AFROTC program. His initial active duty assignment was to the School of Engineering, Air Force Institute of Technology. Having reached the schooling saturation level, he eagerly awaits introduction to "the real Air Force."

Permanent address: Route 1
Cosby, TN 37722

UNCLASSIFIED

SECURITY CLASSIFICATION OF THIS PAGE

REPORT DOCUMENTATION PAGE

1a. REPORT SECURITY CLASSIFICATION Unclassified		1b. RESTRICTIVE MARKINGS	
2a. SECURITY CLASSIFICATION AUTHORITY		3. DISTRIBUTION/AVAILABILITY OF REPORT Approved for public release; distribution unlimited	
2b. DECLASSIFICATION/DOWNGRADING SCHEDULE		4. PERFORMING ORGANIZATION REPORT NUMBER(S) AFIT/GEP/GNE/85M-10	
4. PERFORMING ORGANIZATION REPORT NUMBER(S)		5. MONITORING ORGANIZATION REPORT NUMBER(S)	
6a. NAME OF PERFORMING ORGANIZATION School of Engineering	6b. OFFICE SYMBOL (If applicable) AFIT/EN	7a. NAME OF MONITORING ORGANIZATION	
6c. ADDRESS (City, State and ZIP Code) Air Force Institute of Technology Wright-Patterson AFB, OH 45433		7b. ADDRESS (City, State and ZIP Code)	
8a. NAME OF FUNDING/SPONSORING ORGANIZATION AF Medical Center	8b. OFFICE SYMBOL (If applicable) SGHRT	9. PROCUREMENT INSTRUMENT IDENTIFICATION NUMBER	
8c. ADDRESS (City, State and ZIP Code) USAF Med. Center Wright-Patterson AFB, OH 45433		10. SOURCE OF FUNDING NOS.	
11. TITLE (Include Security Classification) See Box 19		PROGRAM ELEMENT NO.	PROJECT NO.
12. PERSONAL AUTHOR(S) Justin M. Keller, B.S., 2 Lt, USAF		TASK NO.	WORK UNIT NO.
13a. TYPE OF REPORT MS Thesis	13b. TIME COVERED FROM _____ TO _____	14. DATE OF REPORT (Yr., Mo., Day) March 1985	
15. PAGE COUNT 88		16. SUPPLEMENTARY NOTATION	
17. COSATI CODES		18. SUBJECT TERMS (Continue on reverse if necessary and identify by block number)	
FIELD	GROUP	SUB. GR.	
06	12	Radiation Therapy, Tissue Compensation	
	18	Beam Modification	
19. ABSTRACT (Continue on reverse if necessary and identify by block number)			
<p>Title: BEAM MODIFICATION FOR CANCER RADIATION THERAPY</p> <p>Thesis Chairman: Dr. George John</p> <p style="text-align: right;"><i>John Walker</i> (7) afit/r <small>Approved for public release: 12W APR 1984 AFIT/ENP Education, Training and Professional Development Air Force Institute of Technology (AFIT) Wright-Patterson AFB OH 45433</small></p>			
20. DISTRIBUTION/AVAILABILITY OF ABSTRACT UNCLASSIFIED/UNLIMITED <input checked="" type="checkbox"/> SAME AS RPT. <input type="checkbox"/> DTIC USERS <input type="checkbox"/>		21. ABSTRACT SECURITY CLASSIFICATION UNCLASSIFIED	
22a. NAME OF RESPONSIBLE INDIVIDUAL George John, PhD.		22b. TELEPHONE NUMBER (Include Area Code) 513-255-4498	22c. OFFICE SYMBOL AFIT-ENP

UNCLASSIFIED

SECURITY CLASSIFICATION OF THIS PAGE

A method for designing radiation therapy beam modifiers is proposed. The design is based on a calculated dose distribution in the patient from an unmodified treatment beam. The modifier alters the beam before it reaches the patient in a way that yields the desired dose profile at the tumor. The design can be generalized to include any modifier material and any beam energy. The design was applied to an anthropomorphic phantom and verified using thermoluminescent dosimetry. The modifier was constructed of $\frac{1}{2}$ inch square aluminum blocks. The dose distribution in the phantom, with and without beam modification, was measured. The modified dose profile approaches the desired distribution (maximum deviation of + or - 5%). Procedures for improving the results are suggested for further work.

UNCLASSIFIED

SECURITY CLASSIFICATION OF THIS PAGE

END

FILMED

7-85

DTIC